Acknowledgements

This work was supported by The Thailand Research Fund (TRF).

References

- 1. Xu, Y. Ferroelectric Materials and Their Applications. North-Holland, 1991.
- Moon, J., Kerchner, J. A., LeBleu, J., Morrone, A. A. and Adair, J. H., J. Am. Ceram. Soc., 1997, 80, 2613.
- 3. Shirane, G., Axe, J. D. and Harad, J., *Physical Review B*, 1970, **2**(1), 155.
- 4. Shirane, G., Pepinsky, R. and Frazer, B. C., *Acta Cryst.*, 1956, **9**, 131.

- 5. Ueda, I. and Ikegami, S., Jpn. J. Appl. Phys., 1968, 7, 236.
- 6. Shirasaki, S., Solid State Commun., 1971, 9, 1217.
- 7. Levinson, L. M., Electronic Ceramics. New York, 1988.
- 8. Kim, J., Jun, M. C. and Hwang, S. C., J. Am. Cerm. Soc., 1999, 82, 289.
- 9. Moon, J., Li, T., Randall, C. A. and Adair, J. H., J. Mater. Res., 1997, 12, 189.
- 10. Fox, G. R. and Breval, R. E., J. Mater. Res., 1991, 26, 2566.
- Idrissi, H., Aboujalil, A. and Durand, B., J. Eur. Ceram. Soc., 1999, 19, 1997.
- 12. Lu, C. and Xu, Y., Mater. Lett., 1996, 27, 13.
- Pillai, C. G. S. and Ravindran, P. V., Thermochimica Acta, 1996, 278, 109
- Wang, H. C. and Schulze, W. A., J. Am. Ceram. Soc., 1990, 73, 825
- Gupta, S. M. and Kulkarni, A. R., J. Mater. Res., 1995, 10, 953

International Journal of Modern Physics B Vol. 20, No. 17 (2006) 2415–2424 © World Scientific Publishing Company



EFFECT OF SINTERING TEMPERATURE ON DENSIFICATION AND DIELECTRIC PROPERTIES OF ${\rm Pb}({\rm Zr}_{0.44}{\rm Ti}_{0.56}){\rm O}_3 \ {\rm CERAMICS}$

R. YIMNIRUN*, R. TIPAKONTITIKUL and S. ANANTA

Department of Physics, Faculty of Science, Chiang Mai University, Chiang Mai, 50200, Thailand *rattikornyimnirun@yahoo.com

Received 31 October 2005

In this study, lead zirconate titanate (Pb(Zr_{0.44}Ti_{0.56})O₃) ceramics were fabricated with a mixed oxide synthetic route of lead oxide (PbO) and zirconium titanate (ZrTiO₄) precursors. The effects of sintering temperature on phase formation, densification and dielectric responses of the ceramics have been investigated using XRD, SEM, EDX and dielectric measurement techniques. The densification of the PZT ceramics with density of 97% theoretical density can be achieved with appropriate sintering condition without any sintering additives. The optimized sintering condition has been identified as 1225° C for 4 h. More importantly, the dielectric properties are found to improve with increasing sintering temperature and grain size. However, when sintered over 1250° C, the dielectric properties of the ceramics are seen to deteriorate as a result of PbO vaporization, ZrO₂ segregations and porosity.

Keywords: Lead zirconate titanate; PZT; sintering; densification; dielectric properties.

1. Introduction

Lead zirconate titanate ceramics, $Pb(Zr_xTi_{1-x})O_3$ or PZT, have been widely investigated on their electrical properties for several decades. As a prototype of piezoelectrics, PZT ceramics exhibit good dielectric and piezoelectric properties, especially the compositions near the morphotropic phase boundary (MPB). Therefore, they have been exploited in several commercial applications such as ultrasonics, buzzers, actuators and transducers. In addition, the compositions in the vicinity of MPB, generally identified as 52/48 for Zr/Ti ratio, have also been extensively investigated. This is clearly a result of enhanced properties of the compositions, which have been attributed to the coexistence of tetragonal and rhombohedral phases. More recently, the reports by Noheda $et\ al$. have also identified that the presence of the monoclinic distortion is the origin of the unusually high piezoelectric response of PZT compositions near the MPB.

^{*}Corresponding author.

The stoichiometry and densification behavior of the oxide ceramics, which are greatly influenced by sintering conditions, are known to be the key factors for ensuring good electrical properties.⁴ PZT compositions are commonly sintered at high temperatures in the range 1100–1300°C. This creates problems with vaporization of PbO during sintering and possible lead deficiency which may cause segregation of a ZrO₂ phase or a formation of unwanted phases.⁸ This may affect the electrical properties of the material. The B-site precursor method is one the techniques developed to counteract the problem.⁹ In this method, the high temperature phase of ZrTiO₄ is first formed before reacting with PbO to form PZT at lower temperature. Furthermore, the microstructure features such as grain size, grain boundary, density, porosity, and homogeneity markedly influence the electrical characteristics of sintered piezoelectric ceramics. ¹⁰ Kakegawa et al. ¹¹ reported that the dielectric constant of PZT ceramics depends on their chemical compositions. The room temperature dielectric constant of PZT ceramics was found to decrease with increasing grain size, while, on the other hand, the maximum dielectric constant of Pb(Zr_{0.52}Ti_{0.48})O₃ ceramics increased as the grain size decreased. ¹² Generally, the grain size of PZT ceramics increases with the sintering temperature and dwell time. 13,14 Therefore, it could be intuitively expected that the electrical properties of the PZT ceramics would be greatly influenced by the sintering parameters. In this study, the effects of sintering temperature on the densification and the dielectric properties of the sintered PZT ceramics prepared by the Bsite precursor method were investigated. In stead of the typical MPB composition of Pb(Zr_{0.52}Ti_{0.48})O₃, which have been extensively studied, ^{1,3,4,12} the tetragonal composition of Pb(Zr_{0.44}Ti_{0.56})O₃ was chosen in this study. This would extend an understanding on the processing-composition-properties relationships in PZT ceramics.

2. Materials and Methods

PZT powders were synthesized by a modified two-stage mixed oxide route. The $\rm ZrTiO_4$ precursor powders were mixed with PbO for 24 h and calcined at 800°C for 2 h, as reported earlier. Ceramic fabrication was achieved by adding 3 wt% polyvinyl alcohol (PVA) binder, then uniaxially pressed to form a green pellet of 10 mm diameter and 2 mm thick. The pellets were placed inside a closed alumina crucible covered with lead zirconate (PbZrO₃) powder to compensate the PbO volatilization and then sintered at various temperatures for 4 h with constant heating/cooling rates of 10°C/min. During the heating, the temperature was maintained at 500°C for 2 h to burn out the PVA binder. The pellets were subjected to bulk densities measurement with Archimedes method.

Finally, the XRD, SEM and dielectric properties measurement were carried out. X-ray diffraction analysis of the sintered samples was carried out at room temperature using $CuK\alpha$ radiation (40 kV) on X' Pert X-ray diffractometer. Scanning electron microscopy (JEOL, JSM5910LV) was employed and the average grain size

 $(\Phi_{\rm av})$ of samples was determined using the linear interception method. For electrical measurement, the as-sintered samples were polished to parallel surfaces. The major faces of the samples were coated with conductive Pt paint, and then heat cured at 700°C for 1 h to ensure that the electrodes were completely adhered to the ceramic. The dielectric properties were monitored as a function of temperatures (25–400°C) at a measuring frequency of 1 kHz using a computer controlled impedance analyzer (HP Model 4284A).

3. Results and Discussion

The densification of the PZT at various sintering temperatures is investigated. The change in density versus the sintering temperature (1100–1320 $^{\circ}\mathrm{C})$ is shown in Fig. 1. In the sintering temperature range of 1100–1250°C, the density increases with increasing temperature. Further increase in the sintering temperature to 1320°C leads to the decrease of the density. This feature creates a maximum density value of about 97% of theoretical density which is comparable to the value reported by Wang et al. 15 where Li₂CO₃, Bi₂O₃ and CuO were used as sintering aids. The increasing density with rising sintering temperature up to 1250°C may be explained by the enhanced densification as the sintering of PZT is normally found at 1200°C. ¹⁶ Further increase in the sintering temperature causes a decrease in density values. This may be attributed to the loss of lead oxide at high sintering temperatures, which is similar to the results found in other Pb-based perovskite systems. 17,18

XRD patterns of PZT ceramics sintered at various temperatures are plotted in Fig. 2. The strongest reflections in the majority of the XRD patterns can be identified as the perovskite phase of the composition Pb(Zr_{0.44}Ti_{0.56})O₃, which could be matched with JCPDS file 50-346. To a first approximation, this phase has a tetragonal perovskite-type structure in space group P4mm (No. 99), with cell

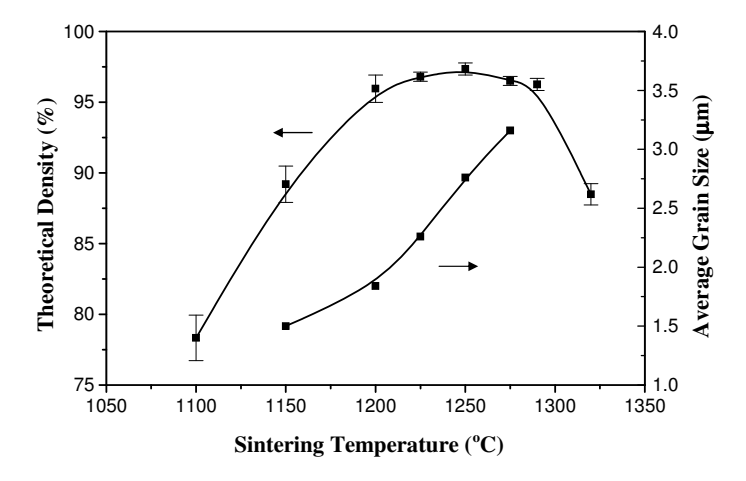


Fig. 1. Variation of density and grain size with sintering temperature for the PZT ceramics.

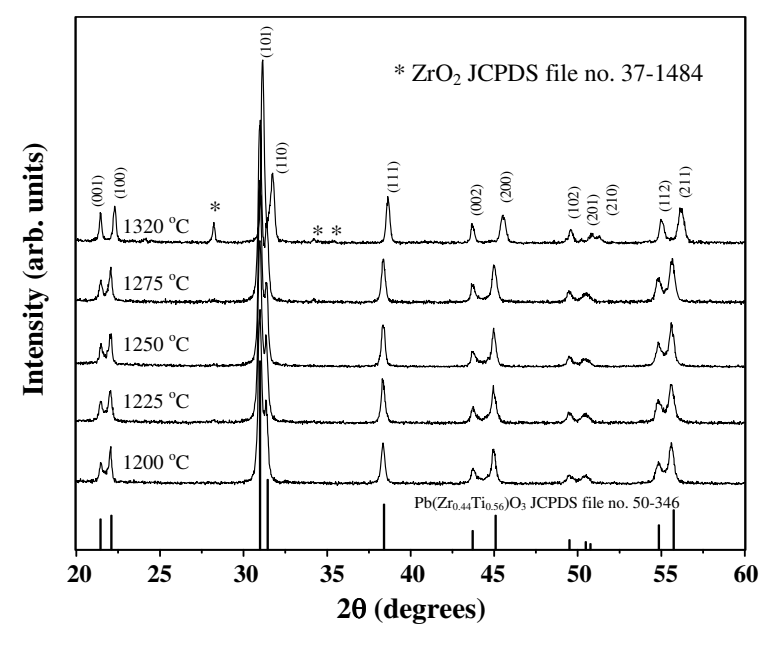


Fig. 2. XRD patterns of the PZT ceramics sintered at various temperatures.

parameters a=401 pm and c=414 pm, respectively.¹⁹ However, for the sample sintered at 1320°C, some additional reflections (marked by *) are observed, and these can be identified as presence of ZrO₂ (JCPDS file 37-1484). This phase has a monoclinic structure with cell parameters a=531.2, b=521.2, c=514.7 pm and $\beta=99.218^{\circ}$ in space group P21/a (No. 14).²⁰ Due to no trace of ZrO₂ has been observed for the samples sintered at the temperatures below 1320°C, it is believed that the consequence of PbO evaporation is an apparently favorable factor in facilitating the occurrence of ZrO₂ at a higher sintering temperature.^{21,22}

Microstructure development was investigated by scanning electron microscopy (SEM). Free surface micrographs of PZT ceramics sintered at various temperatures from $1150-1320^{\circ}$ C are shown in Fig. 3. Also depicted in Fig. 1, the results indicate that grain size tends to increase with sintering temperatures in the temperature range $1150-1275^{\circ}$ C that sees the grain size of the samples changed from 1.5 to 3.2 μ m, in agreement with a previous work by Hong et al.²³ Similar findings were also reported in Nb-doped PZT and modified PT ceramics.^{24,25} However, the average grain size of PZT sintered at 1320° C cannot be determined from SEM micrograph because of the ZrO₂ segregations that are confirmed by XRD results shown in Fig. 2, which also displays very high degree of porosity. In addition to the PbO evaporation, the presence of ZrO₂ segregations and a porous microstructure is believed to be another cause for the decrease in the ceramic density at high sintering temperature. As will be discussed later, these factors are also responsible for the dielectric behavior of the PZT ceramics.

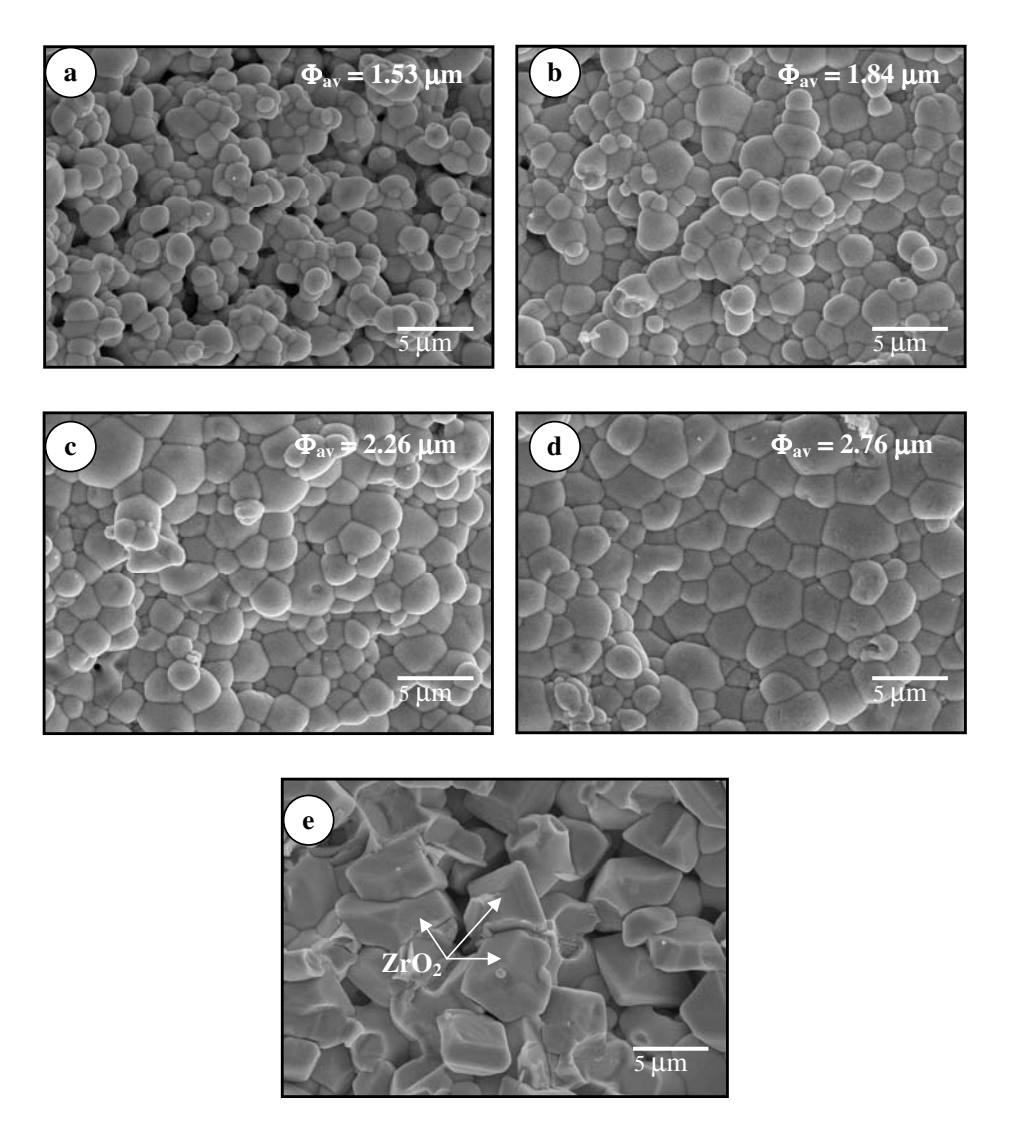


Fig. 3. SEM micrographs of the PZT ceramics sintered at (a) 1150° C, (b) 1200° C, (c) 1225° C, (d) 1250° C and (e) 1320° C.

The variations of dielectric constant (ε_r) and dissipation factor at 1 kHz with sintering temperature are shown in Fig. 4. For all samples in the present work, the Curie temperature is seen independent of the sintering temperature. Similar results have also been reported by other workers. 26,27 The results in Fig. 4 clearly indicate that the dielectric properties of the PZT ceramics depend on the sintering temperature. As listed in Table 1, the maximum value of dielectric constant $(\varepsilon_{r,\text{max}})$ measured at T_C increases from 8250 to 18984 as the sintering temperature increases from 1150-1225°C. Further increase in the sintering temperature to 1275°C results

Fig. 4. Temperature dependence of (a) dielectric constant and (b) dissipation factors at 1 kHz for the PZT ceramics sintered at various temperatures.

in a drop in the values of $\varepsilon_{r,\mathrm{max}}$. to 10378. The opposing trend is observed in the values of the high temperature dielectric loss (tan δ). It should also be noted here that since the dielectric loss in all ceramics increases significantly at high temperature as a result of thermally activated space charge conduction, ²⁸ the values of the high temperature dielectric loss (tan δ) determined at 200°C are listed for comparison. As also listed in Table 1, the similar tendency is also observed for the

Table 1. Physical and dielectric properties of PZT ceramics sintered at various temperatures.

			Dielectric Properties at 1 kHz			
Sintering temperature (°C)	Average grain size (μm)	T_c (°C)	ε_r (25°C)	$\tan \delta$ (25°C)	$ \varepsilon_{r,\text{max}} $ $ (T_C) $	$\tan \delta$ (200°C)
1150	1.53	381	564	0.0072	8250	0.160
1200	1.84	385	638	0.0039	11316	0.145
1225	2.26	380	697	0.0038	18984	0.120
1250	2.76	379	463	0.0042	16524	0.150
1275	3.16	377	397	0.0047	10378	0.265

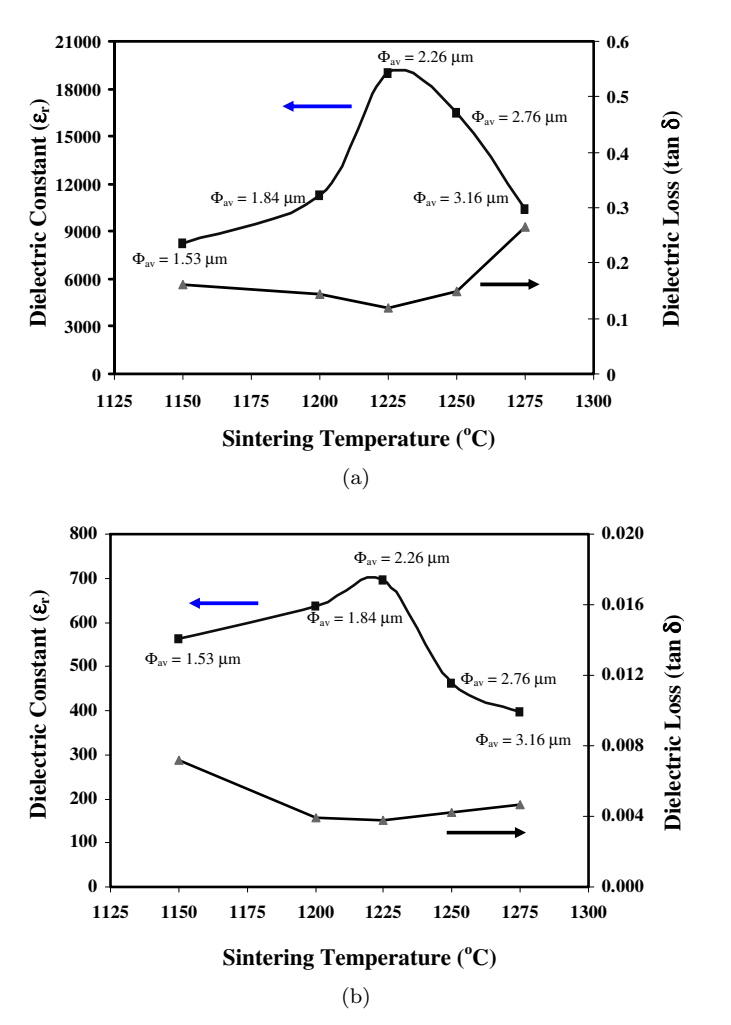


Fig. 5. Variation of (a) maximum dielectric properties and (b) room temperature dielectric properties with sintering temperature for the PZT ceramics.

room temperature dielectric properties. Figure 5 clearly depicts the relationship between the dielectric properties and the sintering temperature. In addition, it is worth noting that the measured values of the dielectric properties in the present work are in good agreement with the previous works on PZT ceramics prepared by different processing techniques. $^{12,29-31}$

By comparing Figs. 1 and 5, the tendency of ε_r values with the sintering temperature is similar to that of density, in good agreement with the report by Kong and Ma,³¹ while the average grain size also increases monotonically with sintering temperatures. Earlier report by Chu et al. 25 also showed similar observations in Nb-doped PZT ceramics. Clearly, the increasing dielectric constant (both at room and Curie temperatures) is due to the increasing density of the ceramics. However, the decreasing room temperature dielectric constant as sintering temperature above 1225° C can be related to the increasing grain size. Kang et al.³² reported that the room temperature dielectric constant decreased with the increasing grain size. Similar results were also reported for BaTiO₃, modified PT and PLZT ceramics.^{24,32,33} On the other hand, an earlier report by Okazaki et al.³⁴ showed that the maximum dielectric constant of PZT ceramics increased with increasing grain size. This is probably because increasing grain size results in reduction of the volume fraction of grain boundaries. The coupling effect between the grain boundaries and the domain wall, which makes domain reorientation more difficult and severely constrains the domain wall motion, is then decreased. This translates to an increase in the domain wall mobility corresponding to an increase in dielectric constant. 12,23,35 In this study, an initial increase of the maximum dielectric constant with the sintering temperature up to 1225°C, as shown in Fig. 5, can be related to the increasing grain size. However, the maximum dielectric constant values of the sintered samples then decrease from 18984 to 10378 as the sintering temperature is increased to 1275°C. This observation may be attributed to microstructure inhomogeneity of the PZT ceramics as a result of PbO deficiency, ZrO₂ precipitation, and porosity at higher sintering temperature. Thus, the higher sintering temperature and the presence of ZrO₂ impurity can significantly reduce the values of the dielectric constant of the PZT ceramics. Finally, it should be emphasized that even though many earlier studies have established a relationship between the dielectric properties and grain size in PZT as well as other perovskite ceramics, this study has shown that other factors such as the sintering conditions, the presence of pores, ZrO₂ and other secondary phases, chemical homogeneity, and Zr/Ti ratio clearly have strong influence on the dielectric properties of the PZT ceramics.

4. Conclusions

 $Pb(Zr_{0.44}Ti_{0.56})O_3$ ceramics were successfully fabricated by employing the modified two-stage mixed oxide route and the effects of the sintering temperature on the densification and dielectric properties were investigated. High density PZT ceramics were obtained for the sintering temperatures about $1200-1250^{\circ}C$. The dielectric

properties of the PZT ceramics are dependent on sintering temperature. It is clear that the dielectric constant increases with increasing sintering temperature and grain size. However, the increasing trends between the density and dielectric properties and the sintering temperature are interrupted when the ceramics are sintered above 1250°C as a result of PbO vaporization, ZrO₂ segregation and porosity.

Acknowledgment

The authors would like to express their gratitude for financial support from the Thailand Research Fund (TRF) and Faculty of Science, Chiang Mai University.

References

- 1. G. H. Haertling, J. Am. Ceram. Soc. 82(4), 797 (1999).
- 2. L. E. Cross, Mater. Chem. Phys. 43, 108 (1996).
- 3. A. J. Moulson and J. M. Herbert, *Electroceramics*, 2nd edn. (Wiley-Interscience, New York, 2003).
- 4. B. Jaffe, W. R. Cook and H. Jaffe, Piezoelectric Ceramics (Academic Press, New York, 1971).
- 5. R. Guo, L. E. Cross, S.-E. Park, B. Noheda, D. E. Cox and G. Shirane, Phys. Rev. Lett. 84(23), 5423 (2000).
- 6. B. Noheda, J. A. Gonzalo, L. E. Cross, R. Guo, S.-E. Park, D. E. Cox and G. Shirane, Phys. Rev. B. 61(13), 8687 (2000).
- 7. B. Noheda, D. E. Cox, G. Shirane, J. A. Gonzalo, L. E. Cross and S.-E. Park, Appl. Phys. Lett. **74**(14), 2059 (1999).
- 8. B. V. Hiremath, A. I. Kingon and J. V. Biggers, J. Am. Ceram. Soc. 66(11), 790 (1983).
- 9. R. Tipakontitikul and S. Ananta, Mater. Lett. 58, 449 (2004).
- 10. Y. Xu, Ferroelectric Materials and Their Applications (Elsevier Science, Amsterdam, 1991).
- 11. K. Kakegawa, J. Mohri, T. Takahashi, H. Yamamura and S. Shirasaki, Solid State Commun. 24, 769 (1977).
- 12. B. M. Jin, J. Kim and S. C. Kim, Appl. Phys. A-Mater. 65, 53 (1997).
- 13. A. Garg and D. C. Agrawal, Mat. Sci. Eng. B-Solid. 56, 46 (1999).
- 14. E. K. Goo, R. K. Mishra and G. Thomas, J. Am. Ceram. Soc. 64(6), 517 (1981).
- 15. X. X. Wang, K. Murakami, O. Sugiyama and S. Kaneko, J. Eur. Ceram. Soc. 21, 1367 (2001).
- 16. A. Megriche and M. Troccaz, Mater. Res. Bull. 33, 569 (1998).
- 17. E. R. Nielsen, E. Ringgaard and M. Kosec, J. Eur. Ceram. Soc. 22, 1847 (2002).
- 18. A. Boutarfaia, Ceram. Inter. 26, 583 (2000).
- 19. Powder diffraction File no. 50-346. International Centre for Diffraction Data, Newton Square, PA, 2000.
- 20. Powder diffraction File no. 37-1484. International Centre for Diffraction Data, Newton Square, PA, 2000.
- 21. S. Fushimi and T. Ikeda, J. Am. Ceram. Soc. 50, 129 (1967).
- 22. Z. Branković, G. Branković and J. A. Varela, J. Mater. Sci. 14, 37 (2003).
- 23. Y.-S. Hong, H.-B. Park and S.-J. Kim, J. Eur. Ceram. Soc. 18, 613 (1998).
- 24. T. Y. Chen, S. Y. Chu and Y. D. Juang, Sensor. Actuat. A-Phys. 102, 6 (2002).
- 25. S. Y. Chu, T. Y. Chen and I. T. Tsai, Integr. Ferroelectr. 58, 1293 (2003).

- 26. L. B. Kong, W. Zhu and O. K. Tan, Mater. Lett. 42, 232 (2000).
- G. Fantozzi, A. Bouzid, E. M. Bourim and M. Gabbay, J. Eur. Ceram. Soc. 25(13), 3213 (2005).
- 28. R. Yimnirun, S. Ananta and P. Laoratanakul, Mat. Sci. Eng. B-Solid. 112, 79 (2004).
- 29. H. Ouchi, M. Nishida and S. Hayakawa, J. Am. Ceram. Soc. 49(11), 577 (1966).
- 30. E. R. Nielsen, E. Ringgaard and M. Kosec, J. Eur. Ceram. Soc. 22, 1847 (2002).
- 31. L. B. Kong and J. Ma, Mater. Lett. 51, 95 (2001).
- 32. B. S. Kang, G. C. Dong and S. K. Choi, J. Mater. Sci. Lett. 9, 139 (1998).
- 33. K. Kinoshita and A. Yamaji, J. Appl. Phys. 47(1), 371 (1976).
- 34. K. Okazaki and K. Nagata, J. Electron. Commun. Soc. Jpn. C. 53, 815 (1970).
- 35. P. Ravindranathan, S. Komarneni, A. S. Bhalla and R. Roy, J. Am. Ceram. Soc. 74, 2996 (1991).







materials letters

Materials Letters 59 (2005) 3732 - 3737

www.elsevier.com/locate/matlet

Dielectric properties of solid solutions in the lead zirconate titanate—barium titanate system prepared by a modified mixed-oxide method

Wanwilai Chaisan ^{a,*}, Rattikorn Yimnirun ^a, Supon Ananta ^a, David P. Cann ^b

^aDepartment of Physics, Faculty of Science, Chiang Mai University, Chiang Mai, Thailand ^bMaterials Science and Engineering Department, Iowa State University, Ames, IA, USA

> Received 13 January 2005; accepted 30 June 2005 Available online 22 July 2005

Abstract

Ceramic solid solutions within the system $(1-x)Pb(Zr_{0.52}Ti_{0.48})O_3-xBaTiO_3$, where x ranged from 0.0 to 1.0, were prepared by a modified mixed-oxide method. The crystal structure, microstructure and dielectric properties of the ceramics were investigated as a function of composition via X-ray diffraction (XRD), scanning electron microscopy (SEM) and dielectric spectroscopy. While pure BT and PZT ceramics exhibited sharp phase transformation expected for normal ferroelectrics, the (1-x)PZT-xBT solid solutions showed that with increasing solute concentration (BT or PZT), the phase transformation became more diffuse. This was primarily evidenced by an increased broadness in the dielectric peak, with a maximum peak width occurring at x=0.4. © 2005 Elsevier B.V. All rights reserved.

Keywords: Dielectric properties; Barium titanate (BT); Lead zirconate titanate (PZT)

1. Introduction

Currently lead-based perovskite ferroelectric ceramics are widely applied in multilayer capacitors and sensors because of their excellent electrical properties [1]. Many of these applications require materials with superior dielectric and piezoelectric properties. Both BaTiO₃ (BT) and Pb(Zr,Ti)O₃ (PZT) are among the most common ferroelectric materials and have been studied extensively since the late 1940s [2,3]. These two ceramics have distinct characteristics that make each ceramic suitable for different applications. The compound Pb(Zr_{0.52}Ti_{0.48})O₃ (PZT) has great piezoelectric properties which can be applied in transducer applications. Furthermore, it has a high $T_{\rm C}$ of 390 °C which allows piezoelectric devices to be operated at relatively high temperatures. Barium

titanate (BT) is a normal ferroelectric material which exhibits a high dielectric constant, a lower $T_{\rm C}$ (~120 °C) and better mechanical properties [1-3]. However, sintering temperature of BT is higher than PZT. Thus, mixing PZT with BT is expected to decrease the sintering temperature of BT-based ceramics, a desirable move towards electrode of lower cost [4]. Moreover, since PZT-BT is not a pure-lead system, it is easier to prepare single phase ceramics with significantly lower amount of undesirable pyrochlore phases, usually associated with lead-based system [5,6]. With their complimentary characteristics, it is expected that excellent properties with preparation ease can be obtained from ceramics in PZT-BT system. In addition, the Curie temperature of PZT-BT system can be engineered over a wide range of temperature by varying the composition in this system. Therefore, this study is aimed at investigating dielectric properties of PZT-BT system over the whole composition range in hope to identify compositions with desirable properties.

E-mail address: wanwilai_chaisan@yahoo.com (W. Chaisan).

^{*} Corresponding author.

BT has been mixed into solid solutions with SrTiO₃ (BST) and with PbTiO₃ (BPT) to adjust the Curie temperature and to optimize the dielectric and piezoelectric response [1,2,7,8]. PZT ceramics are always modified with other chemical constituents, such as Nb and La, to improve the physical properties for specific applications [2,3,9]. Moreover, solid solutions between normal and relaxor ferroelectric materials such as PZN-BT [10], PMN-PZT [11], PZT-PNN [12], PMN-PT [13] and PZN-PT [14] have been widely studied for dielectric applications and to examine the order-disorder behavior. However the superior dielectric properties of these relaxor systems have been associated with the presence of unwanted phase, densification behavior and microstructure development [15]. It is well known that the single phase of relaxor materials is very difficult to prepare and these systems always exhibit high dielectric loss and strong frequency dependence which is not suitable for some applications [2,16]. Even though there have been extensive work on PZT-based and BT-based solid solutions, there are only a few studies on PZT-BT solid solutions [5,6,17]. Chaisan et al. [5] prepared perovskite powders in the whole series of the solid solutions in PZT-BT system. The phase formation characteristics, cell parameters and the degree of tetragonality were examined as a function of composition. It was found that complete solid solutions of perovskite-like phase in the (1-x)PZT-xBT system occurred across the entire composition range. Lattice parameters of the tetragonal phase and of the rhombohedral phase were found to vary with chemical composition. The degree of tetragonality increased, while optimum firing temperatures decreased continuously with decreasing BT content. Moreover, pseudo-binary system of PZN-BT-PZT was previously studied and the effect of processing conditions on the piezoelectric and dielectric properties of this system was also discussed [17].

Thus far, from these literatures, there have been no systematic studies on the dielectric properties of the whole series of PZT-BT compositions. Therefore, as an extension of our earlier work on structural studies of the PZT-BT system [5], the overall purpose of this study is to investigate the dielectric properties of the solid solution between two normal ferroelectrics with the aim of identifying excellent electrical properties within this system. Although the conventional mixed-oxide method has attracted interest to prepare normal ferroelectric PZT and BT materials for many decades, several methods such as mechanical activation [6] and sol-gel-hydrothermal technique [18] still have been developed for better approach. A number of chemical routes has also been used as alternatives [19–21]. However these techniques are more complicated and expensive than the conventional mixed-oxide route, which limits its commercial applicability for mass powder synthesis. In this respect, it is desirable to develop a method based on the mixed-oxide

method for preparation of PZT-BT ferroelectric materials. Therefore, this paper presents the dielectric properties of compositions in the PZT-BT binary system prepared via a modified mixed-oxide method, in which PZT powders are prepared through lead zirconate (PbZrO₃) precursor to eliminate pyrochlore phase usually found in powders from a conventional mixed-oxide method [5].

2. Experimental procedures

The compositions $(1-x)Pb(Zr_{0.52}Ti_{0.48})O_3-xBaTiO_3$ or (1-x)PZT-xBT, where x=0.0, 0.1, 0.3, 0.4, 0.5, 0.7, 0.9and 1.0, were prepared by a modified mixed-oxide method [5]. Reagent grade PbO, ZrO2, TiO2 and BaCO3 powders (Fluka, >99% purity) were used as starting materials. Powder of each end member (PZT and BT) was first formed in order to avoid unwanted pyrochlore phases. For the preparation of BT, BaCO₃ and TiO₂ powders were homogeneously mixed via ball-milling for 24 h with zirconia media in ethanol. The well-mixed powder was calcined at 1300 °C for 2 h in an alumina crucible. With a modified mixed-oxide method [5], the PZT powders were prepared by using a lead zirconate (PbZrO₃) as precursor in order to reduce the occurrence of undesirable phase. Pure PbZrO₃ phase was first formed by reacting PbO with ZrO2 at 800 °C for 2 h. PbZrO3 powder was then mixed with PbO and TiO2 and milled, dried and calcined at 900 °C for 2 h to form single phase PZT. The (1-x)PZT-xBT powders were then formulated from the BT and PZT components by employing the similar mixed-oxide procedure and calcining at various

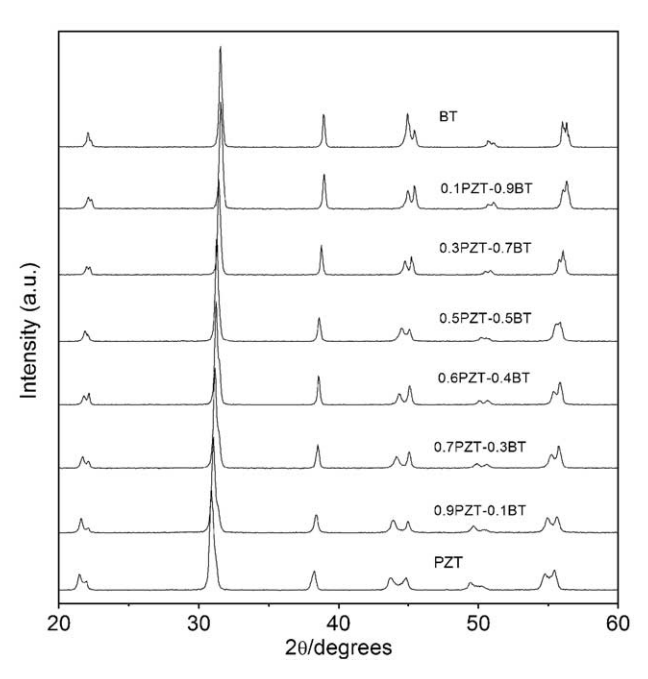


Fig. 1. XRD diffraction patterns of sintered (1-x)PZT-xBT ceramics.

Table 1 Characteristics of (1-x)PZT-xBT ceramics with optimized processing conditions

Compositions	Sintering temperature (°C)	Density (g/cm ³)	Average grain size (μm)
PZT	1100	7.7	2.36
0.9PZT-0.1BT	1200	7.6	2.86
0.7PZT-0.3BT	1200	7.2	1.97
0.6PZT-0.4BT	1250	6.9	2.31
0.5PZT-0.5BT	1250	6.6	3.87
0.3PZT-0.7BT	1250	5.7	3.71
0.1PZT-0.9BT	1300	5.3	5.72
BT	1350	5.8	2.42

temperatures between 900 and 1300 °C for 2 h in order to obtain single phase (1-x)PZT-xBT powders [5].

The calcined (1-x)PZT-xBT powders were then isostatically cold-pressed into pellets with a diameter of 15 mm and a thickness of 2 mm at a pressure of 4 MPa and sintered for 2 h over a range of temperatures between 1050 and 1350 °C depending upon the composition. Densities of sintered ceramics were measured by Archimedes method and X-ray diffraction (XRD using CuK $_{\alpha}$ radiation) was employed to identify the phases formed. The grain morphology and size were directly imaged using scanning electron microscopy (SEM) and the average grain size was determined by using a mean

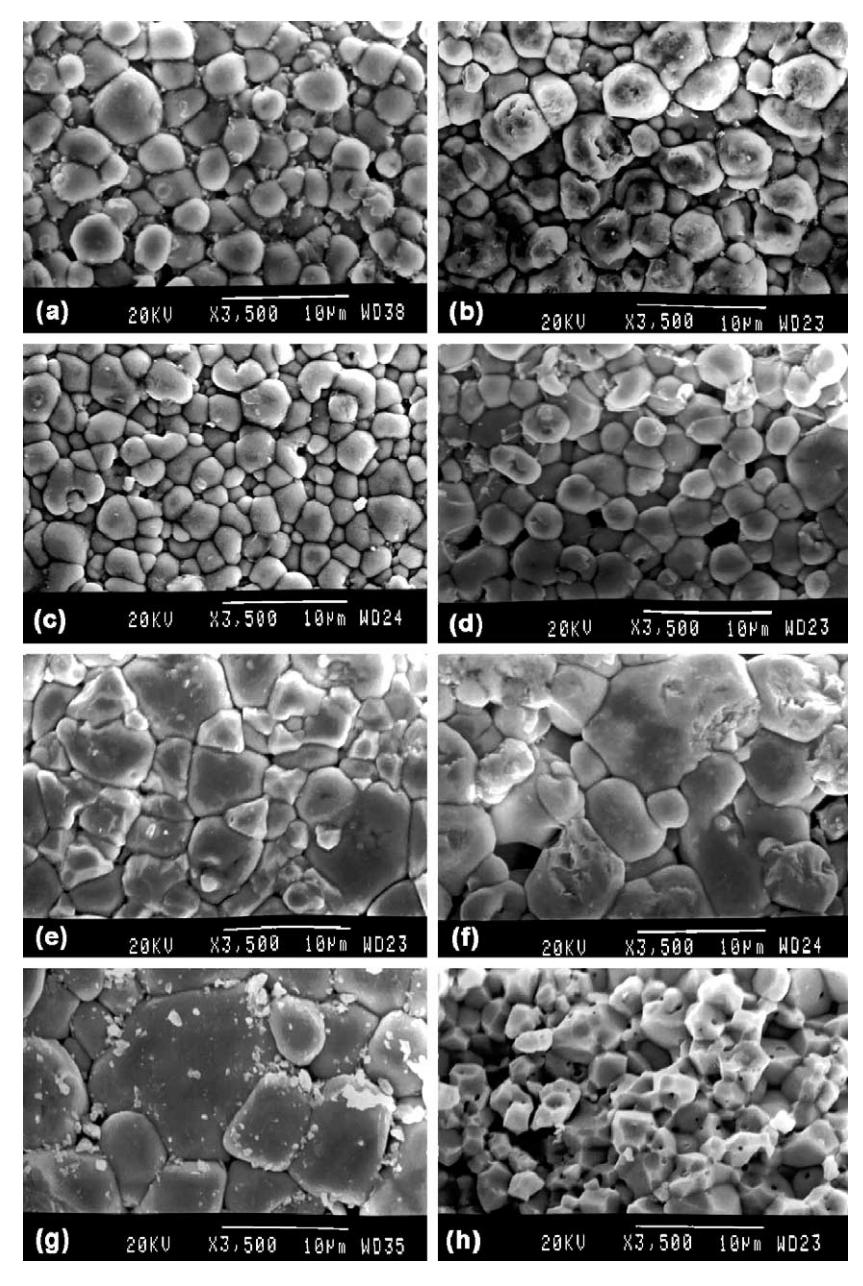


Fig. 2. SEM micrographs of (1-x)PZT-xBT ceramics: (a) PZT, (b) 0.9PZT-0.1BT, (c) 0.7PZT-0.3BT, (d) 0.6PZT-0.4BT, (e) 0.5PZT-0.5BT, (f) 0.3PZT-0.7BT, (g) 0.1PZT-0.9BT and (h) BT.

linear intercept method [22]. For electrical measurements, silver paste was fired on both sides of the polished samples at 550 °C for 30 min as the electrodes. A dimension of ceramics after sintered and polished is about 12.5 mm in diameter and 1 mm in thickness. Dielectric properties of the sintered ceramics were studied as a function of both temperature and frequency. The capacitance was measured with a HP4284A LCR meter in connection with a Delta Design 9023 temperature chamber and a sample holder (Norwegian Electroceramics) capable of high temperature measurement. Dielectric constant (ε_r) was calculated using the geometric area and thickness of the discs.

3. Results and discussion

The phase formation behavior of the sintered (1-x)PZT-xBT ceramics is revealed by XRD as shown in Fig. 1. The BaTiO₃ ceramic sintered at 1350 °C was identified as single phase perovskite having tetragonal symmetry. With increasing PZT content, the diffraction peaks shifted towards lower angle and the diffraction peak around 2θ of $43^{\circ}-46^{\circ}$ was found to split at composition x=0.5. This observation suggests that this composition may lead to a diffuse MPB between the tetragonal and rhombohedral PZT phases [23]. In

this case, the peak of tetragonal phase is much stronger than that of rhombohedral phase. However, the (200) peak splitting for the PZT–BT system exhibited more clearly in powders as reported in our earlier work [5]. Additionally, the PZT–BT ceramics showed single diffraction peaks which indicate good homogeneity and complete solid solution within the (1-x)PZT–xBT system [24]. The pure Pb(Zr_{0.52}Ti_{0.48})O₃ ceramic sintered at 1100 °C showed a co-existence of both tetragonal and rhombohedral phases which can be matched with the JCPDS file no. 33-0784 and 73-2022, respectively.

The optimized sintering temperatures at which ceramics with single phase and highest densification are obtained, densities, and average grain sizes of the sintered (1-x)PZT-xBT ceramics are listed in Table 1. Higher firing temperatures were necessary for compositions containing a large fraction of BT. Compositions with x=0.7 and x=0.9 could not be sintered to sufficient densities and the theoretical densities of ceramics in this range were about 86%-89%. It is possible that volatilization of PbO during firing is the main reason for the failure in preparing dense ceramics over this composition range [25,26]. As shown in Fig. 2, SEM micrographs reveal that the compositions with $0.0 \le x \le 0.4$ exhibit good densification and homogenous grain size. For the compositions with $0.5 \le x \le 0.9$, the grain size varies greatly from 1 to 15 µm and defective grains and some degree of porosity are clearly seen; these matched with the density data. The reason for the variation of grain sizes in this composition range is not clearly understood. However, it can be assumed that since sintering temperatures for highest

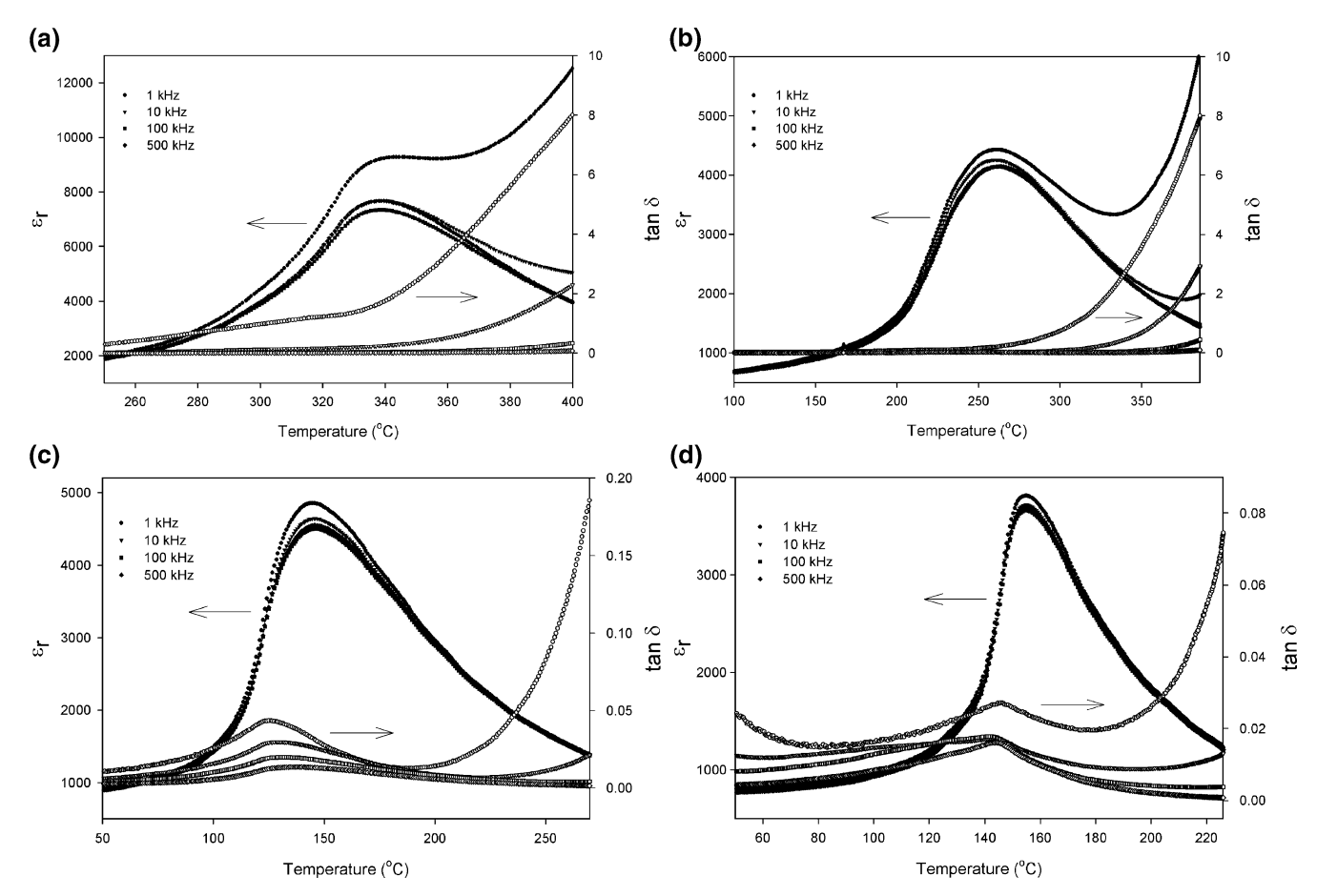


Fig. 3. Temperature and frequency dependence of dielectric properties of (a) 0.9PZT-0.1BT, (b) 0.7PZT-0.3BT, (c) 0.3PZT-0.7BT and (d) 0.1PZT-0.9BT ceramics.

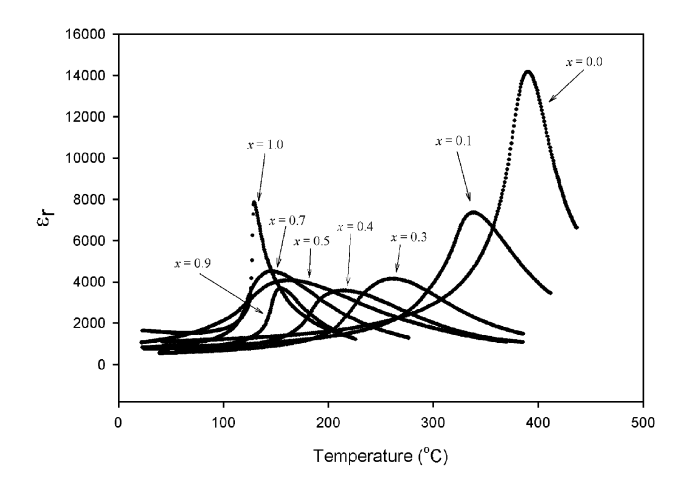


Fig. 4. Temperature dependence of dielectric constant $(\varepsilon_{\rm r})$ of $(1-x){\rm PZT}-x{\rm BT}$ ceramics at 100 kHz.

densification of PZT and BT ceramics are very different (900 °C and 1300 °C, respectively), this could lead to different grain growth behaviors between two phases, hence heterogeneous microstructure [27].

Fig. 3 shows the temperature dependence of dielectric constant $(\varepsilon_{\rm r})$ and dissipation factor (tan δ) at various frequencies for compositions with x=0.1, 0.3, 0.7 and 0.9. All compositions show indication of a diffuse phase transition of dielectric constant with rather weak frequency dependence. In addition, Curie temperatures $(T_{\rm C})$ are also noticeably frequency independent [28]. It should be noted that the dielectric loss tangent of all ceramics increases rapidly at high temperature as a result of thermally activated space charge conduction [11]. The representative temperature dependence of the dielectric constant (ε_r) measured at 100 kHz for (1-x)PZT-xBT samples with $0.0 \le x \le 1.0$ is shown in Fig. 4. The Curie temperatures and maximum dielectric constants of the pure PZT and BT ceramics in this work were, respectively, 390 °C and 14,200 for PZT, and 129 °C and 7800 for BT. Therefore, a solid solution between PZT and BT is expected to show a transition temperature between 390 and 129 °C. The variation of $T_{\rm C}$ with compositions and dielectric data are listed in Table 2. The Curie temperature significantly decreases with increasing BT content up to 50 mol%. However, for the compositions $0.5 \le x \le 0.9$, T_C is not clearly depending on composition and remains at a nearly constant value between 140 and 160 °C. Even though the presence of Pb is known to shift $T_{\rm C}$ to higher temperatures [2,3], the nearly constant T_C with increasing Pb content in the composition with $0.5 \le x \le 0.9$ is likely caused by PbO loss due to the high sintering temperatures required for these compositions [25,26]. For pure PZT, the ε_r

Table 2 Dielectric properties of (1-x)PZT-xBT ceramics

Compositions	T _C (°C)	ϵ_{m}	γ	δ
PZT	390	14,200	1.74	16.1
0.9PZT-0.1BT	338	7300	1.76	16.2
0.7PZT-0.3BT	262	4100	1.86	16.6
0.6PZT-0.4BT	214	3600	1.97	17.1
0.5PZT-0.5BT	162	4100	1.91	17.3
0.3PZT-0.7BT	146	4500	1.74	15.9
0.1PZT-0.9BT	155	3700	1.63	14.4
BT	129	7800	1.16	12.5

peak is sharp and approaches 15,000. However, the $\varepsilon_{\rm r}$ peaks become broader with increasing BT content, and the broadest peak occurs at the x=0.4 composition. It is very interesting to observe that the $\varepsilon_{\rm r}$ peak becomes more sharp as the BT content further increases.

To understand the interesting dielectric behavior of the PZT-BT system, we look at the different behaviors of normal and relaxor ferroelectric. For a normal ferroelectric such as PZT and BT, above the Curie temperature the dielectric constant follows the Curie-Weiss law:

$$\varepsilon = \frac{c}{T - T_0} \tag{1}$$

where c is the Curie constant and T_0 is the Curie–Weiss temperature [2,11,29]. For a ferroelectric with a diffuse phase transition, the following equation:

$$\frac{1}{\varepsilon} \approx (T - T_{\rm m})^2 \tag{2}$$

has been shown to be valid over a wide temperature range instead of the normal Curie-Weiss law (Eq. (1)) [10,30]. In Eq. (2), $T_{\rm m}$ is the temperature at which the dielectric constant is maximum. If the local Curie temperature distribution is Gaussian, the reciprocal permittivity can be written in the form [10,12]:

$$\frac{1}{\varepsilon} = \frac{1}{\varepsilon_{\rm m}} + \frac{(T - T_{\rm m})^{\gamma}}{2\varepsilon_{\rm m}\delta^2} \tag{3}$$

where $\varepsilon_{\rm m}$ is maximum permittivity, γ is diffusivity, and δ is diffuseness parameter. For $(1-x){\rm PZT}{-}x{\rm BT}$ compositions, the diffusivity (γ) and diffuseness parameter (δ) can be estimated from the slope and intercept of the dielectric data shown in Fig. 5, and tabulated in Table 2.

For the PZT-rich ceramics, the values of γ and δ increase with increasing BT content, confirming the diffuse phase transitions in PZT-BT solid solutions. It is clear that the addition of BT raises the degree of disorder in (1-x)PZT-xBT over the compositional range $0.1 \le x \le 0.5$. The highest degree of diffuseness is exhibited in the 0.5PZT-0.5BT ceramic. Similarly, from the BT end member, the values of both γ and δ exhibit the same trend with

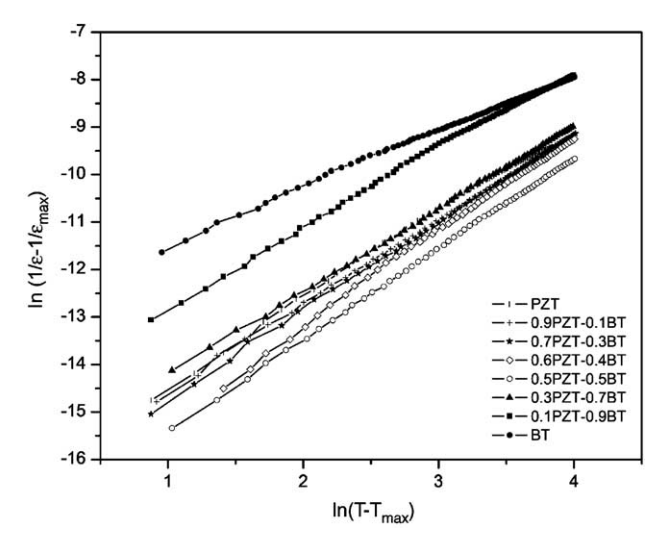


Fig. 5. Plots of $\ln\left(\frac{1}{\varepsilon} - \frac{1}{\varepsilon_m}\right)$ vs. $\ln(T - T_m)$ for (1 - x)PZT-xBT ceramics.

increasing PZT content. This observation indicates that PZT addition also induces disorder in BT-rich compositions. It should also be mentioned here that different dielectric behaviors could also be caused by grain size variation [11]. However, the grain size, as shown in Table 1, in this study does not differ significantly enough to cause such a variation in the dielectric properties. Finally, it should be noted here that with comparison to other solid solution systems, such as PMN-PT, PZN-PT, PZT-PNN [12-14], ceramics in PZT-BT are much easier to prepare with minimized pyrochlore phases, lower dielectric loss and weak frequency dependence.

4. Conclusions

The dielectric properties of solid solutions in the (1-x)PZT-xBT system prepared via the mixed-oxide method are reported. All compositions in this study were single phase perovskite with tetragonal symmetry. The results indicated that the dielectric behavior of pure PZT and BT follows a Curie–Weiss law, while solid solutions of (1-x)PZT-xBT $(0.1 \le x \le 0.9)$ exhibited a diffuse phase transition behavior with a Curie temperature ranging between 390 °C to 129 °C. In (1-x)PZT-xBT solid solutions, the degree of diffuseness increased with increased solute content up to a maximum at x=0.5.

Acknowledgements

This work was supported by the Thailand Research Fund (TRF), Graduate School of Chiang Mai University and the Ministry of University Affairs.

References

- A.J. Moulson, J.M. Herbert, Electroceramics: Materials, Properties, Applications, 2nd edition, John Wiley & Sons, Ltd., 2003, p. 243.
- [2] G.H. Haertling, J. Am. Ceram. Soc. 82 (1999) 797-818.

- [3] B. Jaffe, W.R. Cook, Piezoelectric Ceramics, R.A.N. Publishers, 1971, p. 317.
- [4] J. Chen, Z. Shen, F. Liu, X. Liu, J. Yun, Scr. Mater. 49 (2003) 509-514.
- [5] W. Chaisan, S. Ananta, T. Tunkasiri, Cur. Appl. Phys. 4 (2004) 182–185
- [6] B.K. Gan, J.M. Xue, D.M. Wan, J. Wang, Appl. Phys., A 69 (1999) 433–436
- [7] K. Uchino, Acta Mater. 46 (1998) 3745-3753.
- [8] A.D. Polli, F.F. Lange, C.G. Levi, J. Am. Ceram. Soc. 83 (2000) 873–881.
- [9] H. Jaffe, D.A. Berlincourt, Proc. IEEE 53 (1965) 1372-1386.
- [10] A. Halliyal, U. Kumar, R.E. Newnham, L.E. Cross, Am. Ceram. Soc. Bull. 66 (1987) 671–676.
- [11] R. Yimnirun, S. Ananta, P. Laoratanakul, Mater. Sci. Eng., B, Solid-State Mater. Adv. Technol. 112 (2004) 79–86.
- [12] N. Vittayakorn, G. Rujijanagul, X. Tan, M.A. Marquardt, D.P. Cann, J. Appl. Phys. 96 (2004) 5103–5109.
- [13] K. Babooram, H. Tailor, Z.-G. Ye, Ceram. Int. 30 (2004) 1411-1417.
- [14] J.J. Lima-Silva, I. Guedes, J.M. Filho, A.P. Ayala, M.H. Lente, J.A. Eiras, D. Garcia, Solid State Commun. 131 (2004) 111–114.
- [15] J.P. Guha, J. Eur. Ceram. Soc. 23 (2003) 133-139.
- [16] L.E. Cross, Ferroelectrics 151 (1994) 305-320.
- [17] F. Xia, X. Yao, J. Mater. Sci. 34 (1999) 3341-3343.
- [18] J. Zeng, M. Zhang, Z. Song, L. Wang, J. Li, K. Li, C. Lin, Appl. Surf. Sci. 148 (1999) 137–141.
- [19] R.N. Das, R.K. Pati, P. Pramanik, Mater. Lett. 45 (2000) 743-748.
- [20] A. Abreu, S.M. Zanetti, M.A.S. Oliveira, G.P. Thim, J. Eur. Ceram. Soc. 25 (2005) 743–748.
- [21] R.N. Das, P. Pramanik, Mater. Lett. 40 (1999) 251-254.
- [22] D.G. Brandon, W.D. Kaplan, Microstructural Characterization of Materials, John Wiley & Sons, Ltd., 1999, p. 409.
- [23] A.K. Arora, R.P. Tandon, A. Mansingh, Ferroelectrics 132 (1992) 9.
- [24] B.D. Cullity, Elements of X-ray Diffraction, Addison-Wesley Publishing Company, Inc., 1978, p. 32.
- [25] A. Garg, D.C. Agrawal, Mater. Sci. Eng., B, Solid-State Mater. Adv. Technol. 56 (1999) 46–50.
- [26] C.H. Wang, S.J. Chang, P.C. Chang, Mater. Sci. Eng., B, Solid-State Mater. Adv. Technol. 111 (2004) 124–130.
- [27] Y.-M. Chiang, D.P. Birnie, W.D. Kingery, Physical Ceramics, John Wisley & Sons, Inc., 1997, p. 522.
- [28] T.R. Shrout, J. Fielding, Proc. IEEE Ultrasonics Symposium, 1990, pp. 711–720.
- [29] L.E. Cross, Mater. Chem. Phys. 43 (1996) 108-115.
- [30] R.D. Shannon, C.T. Prewitt, Acta Crystallogr., B Struct. Crystallogr. Cryst. Chem. 25 (1969) 925–945.

Effects of uniaxial stress on dielectric properties lead magnesium niobate—lead zirconate titanate ceramics

Rattikorn Yimnirun, Supon Ananta, Ekarat Meechoowas and Supattra Wongsaenmai

Department of Physics, Faculty of Science, Chiang Mai University, Chiang Mai 50200, Thailand

Received 11 April 2003 Published 18 June 2003 Online at stacks.iop.org/JPhysD/36/1615

Abstract

Effects of uniaxial stress on the dielectric properties of ceramics in lead magnesium niobate–lead zirconate titanate (PMN–PZT) system are investigated. The ceramics with a formula $(x)\text{Pb}(\text{Mg}_{1/3}\text{Nb}_{2/3})\text{O}_3-(1-x)\text{Pb}(\text{Zr}_{0.52}\text{Ti}_{0.48})\text{O}_3$ or (x)PMN-(1-x)PZT when $x=0.0,\,0.1,\,0.3,\,0.5,\,0.7,\,0.9,\,$ and 1.0 are prepared by a conventional mixed-oxide method. Phase formation behaviour and microstructural features of these ceramics are studied by x-ray diffraction and scanning electron microscopy methods, respectively. The dielectric properties under the uniaxial stress of the PMN–PZT ceramics are observed at stress levels up to 5 MPa using a uniaxial compressometer. It is found that with increasing applied stress the dielectric constant of the PZT-rich compositions increases slightly, while that of the PMN-rich compositions decreases. On the other hand, the dielectric loss tangent for most of the compositions first rises and then drops with increasing applied stress.

1. Introduction

Lead magnesium niobate ($Pb(Mg_{1/3}Nb_{2/3})O_3$ or PMN) and lead zirconate titanate $(Pb(Zr_{1-x}Ti_x)O_3 \text{ or } PZT)$ ceramics are widely used in devices like piezoelectric actuators and electromechanical transducers [1-3]. These two types of ceramics possess distinct characteristics that, in turn, make each ceramic suitable for different applications. prototypic relaxor ferroelectric, PMN has advantages of having broader operating temperature range, especially over the room temperature range. This is a direct result of a diffuse paraelectric-ferroelectric phase transition in the vicinity of room temperature. In addition, as a result of their unique microstructure features PMN ceramics exhibit low loss and non-hysteretic characteristics. However, the PMN ceramics have relatively low electromechanical coupling coefficients, as compared to PZT. This is the main reason for rather unsuccessful applications of PMN ceramics in actuators and transducers. In contrast to PMN, PZT ceramics have found several actuator and transducer applications due to their high electromechanical coupling coefficients [1, 2]. However, PZT ceramics are fairly lossy as a result of their highly hysteretic This makes them unsuitable for applications that require high delicacy and reliability. Furthermore, PZT ceramics normally have very high Curie temperature ($T_{\rm C}$) in the vicinity of 400°C. Usually, many applications require that $T_{\rm C}$ be close to ambient temperature. Therefore, there is a general interest to reduce the $T_{\rm C}$ of PZT ceramics to optimize their uses. Forming a solid-solution of PZT and relaxor ferroelectrics has been one of the techniques employed to improve the properties of ferroelectric ceramics. With the complementary features of PMN and PZT, it is of special interest to investigate a solid-solution of PMN–PZT ceramics, which is expected to possess more desirable features than single-phase PMN and PZT [2, 4–6].

Furthermore, these ceramics are often subjected to external mechanical loading when used in specific applications, such as in acoustical transducers [7, 8]. A prior knowledge of how the material properties change under different load conditions is crucial for proper design of a device and for suitable selection of materials for a specific application. Despite this fact, material constants used in any design calculation are often obtained from a stress-free measuring condition, which in turn may lead to incorrect or inappropriate actuator and transducer designs [9–11]. It is therefore important to determine the properties of these materials as a function of applied

stress. Previous investigations on the stress-dependent dielectric and electrical properties of other ceramic systems, such as PZT and PMN–PT have clearly emphasized the importance of the subject [12, 13]. However, there has been no report on the study on the PMN–PZT system. Therefore, this study is undertaken to investigate the influences of the uniaxial stress on the dielectric properties of ceramics in PMN–PZT ceramic composites.

2. Experiments and measurements

The $Pb(Mg_{1/3}Nb_{2/3})O_3$ – $Pb(Zr_{0.52}Ti_{0.48})O_3$ ceramic composites are prepared from PMN and PZT powders by a mixed-oxide method. Perovskite-phase PMN powders are obtained via the well-known columbite method [14]. PZT powders, on the other hand, are prepared by a more conventional mixed-oxide method.

The columbite method is employed in preparing a perovskite-phase PMN. In this method, the magnesium niobate powders are first prepared by mixing starting MgO (>98%) and Nb₂O₅ (99.9%) powders and then calcining the mixed powders at 1050°C for 2.5 h. This yields a so-called columbite powder (MgNb₂O₆). The columbite powders are subsequently ball-milled with PbO (99%) for 24 h. The mixed powders are calcined at 800°C for 2.5 h to form a perovskite-phase PMN. With a more conventional oxide-mixing route, PZT powders are prepared from reagent-grade PbO (99%), ZrO₂ (99%), and TiO₂ (98.5%) starting powders. These powders are ball-milled for 24 h and later calcined at 850°C for 2 h.

The (x)Pb $(Mg_{1/3}Nb_{2/3})O_3-(1 - x)$ Pb $(Zr_{0.52}Ti_{0.48})O_3$ (when x = 0.0, 0.1, 0.3, 0.5, 0.7, 0.9, and 1.0) ceramic composites are prepared from the starting PMN and PZT powders by a mixed-oxide method at various processing conditions. Initially, the PMN and PZT powders for a given composition are weighed and then ball-milled in ethanol for 24 h. After the drying process, the mixed powders are pressed hydraulically to form disc-shaped pellets 15 mm in diameter and 2 mm thick, with 5 wt.% polyvinyl alcohol (PVA) as a binder. The pellets are stacked in a covered alumina crucible filled with PZ powders to prevent lead loss. Finally, the sintering is carried out at a sintering temperature for 2h with $5 \min {^{\circ}}C^{-1}$ heating and cooling rates. The firing profile includes a 1 h dwell time at 500°C for binder burnout process to complete. For optimization purpose, the sintering temperature is varied between 1000°C and 1300°C depending upon the compositions.

The densities of the sintered ceramics are measured by the Archimedes method. The firing shrinkage is determined from the dimensions of the specimens before and after the sintering process. The phase formations of the sintered specimens are studied by an x-ray diffractometer (Philips analytical). The microstructure analyses are undertaken by a scanning electron microscopy (SEM: JEOL Model JSM 840A). Grain size is determined from SEM micrographs by a linear intercept method. For dielectric property characterizations under a uniaxial stress, the sintered samples are lapped to obtain parallel faces, and the faces are then coated with silver paint as electrodes. The samples are heat-treated at 750°C for 12 min to ensure the contact between the electrodes and the ceramic surfaces. The samples are subsequently poled in a silicone

oil bath at a temperature of 120°C by applying a dc field of 25 kV cm⁻¹ for 30 min and field-cooled to room temperature.

To study the effects of the uniaxial stress on the dielectric properties, the uniaxial compressometer is constructed. The details of the system are described elsewhere [15]. The dielectric properties are measured through spring-loaded pins connected to the LCZ-meter (Hewlett Packard, model 4276A). The capacitance and the dielectric loss tangent are determined at frequency of 1 kHz and room temperature (25°C). The dielectric constant is then calculated from a parallel-plate capacitor equation, e.g. $\varepsilon_r = Cd/\varepsilon_0 A$, where C is the capacitance of the sample, d and A are the thickness and the area of the electrode, respectively, and ε_0 is the dielectric permittivity of vacuum $(8.854 \times 10^{-12} \,\mathrm{Fm}^{-1})$. Though the hysteretic behaviour is expected in the materials, as seen in other ferroelectric materials [12], it should be mentioned that with the limitation of the current design of the uniaxial compressometer the reversibility of the dielectric properties with stress is not obtainable in this experiment. The modification of the experimental set-up to measure the reversibility is underway and the results will be presented in future publications.

3. Results and discussion

The optimized density of sintered (x)PMN–(1 - x)PZT ceramics is listed in table 1. It is observed that the compositions with x = 0.1 and 0.3 show relatively lower density than other compositions. This suggests that the addition of a small amount of PMN to the PMN-PZT compositions results in a significant decrease in the density of the ceramics. Further addition of PMN into the compositions increases the density again. A similar result was reported in a previous investigation [4]. The SEM investigations (shown later in figure 2) reveal supporting evidences that the ceramics with these two compositions contain very small and loosely bonded grains. It should, however, be noted that the composition with x = 0.1, which contains sub-micron size grains, is not well sintered. Clearly, this is a reason for the much lower density in this composition. As shown in table 1, the average grain size of all the mixed compositions is much smaller than that of the pure PZT and PMN materials. The reason for the changes of the density and the smaller grain sizes in the mixed compositions is not clearly understood, but this may be a result of PMNs role as a grain-growth inhibitor in the PMN-PZT composites. More importantly, it should be pointed out that dense ceramics

Table 1. Characteristics of PMN–PZT ceramics with optimized processing conditions.

Ceramic	Density (g cm ⁻³)	Firing shrinkage (%)	Grain size range (µm)	Average grain size (µm)
PZT	7.59 ± 0.11	33.5 ± 1.1	2-7	5.23
0.1PMN-0.9PZT	6.09 ± 0.11	18.6 ± 0.1	0.5-2	0.80
0.3PMN-0.7PZT	7.45 ± 0.10	30.8 ± 2.7	0.5 - 3	1.65
0.5PMN-0.5PZT	7.86 ± 0.05	38.3 ± 0.1	0.5 - 5	1.90
0.7PMN-0.3PZT	7.87 ± 0.07	40.4 ± 0.9	1-4	1.40
0.9PMN-0.1PZT	7.90 ± 0.09	38.8 ± 0.1	1-4	1.50
PMN	7.82 ± 0.06	39.9 ± 0.6	2–4	3.25

for PMN-PZT composites are very difficult to obtain as a result of a narrow range of sintering behaviour of PMN material [4].

The phase formation behaviour of the sintered ceramics is revealed by an x-ray diffraction (XRD) method. The XRD patterns, shown in figure 1, show that the sintered ceramics are mainly in perovskite phase. From the XRD pattern, PZT ceramic is identified as a single-phase material with a perovskite structure having tetragonal symmetry, while PMN ceramic is a perovskite material with a cubic symmetry [16]. All PMN-PZT ceramic composites exhibit pseudocubic crystal structure, as reported in previous investigations [4, 5, 15]. However, some impurity phases (Pb₂Nb₂O₇ and MgO) are also present on the XRD patterns of the composites with x > 0.1. A large amount of the secondary pyrochlore phase (Pb₂Nb₂O₇) is clearly present on the SEM micrographs (figures 2(d)–(f)). These impurities phases are believed to precipitate mostly on the surface areas of the specimens [17]. Further XRD investigation at different depths of the specimen reveals that the impurities diminish in the interior areas of the specimens.

The microstructures of the specimens sintered at 1150°C are observed with the SEM, as shown in figure 2. Clearly, the morphology of the grains is composition-dependent. PZT and PMN ceramics exhibit more uniform microstructure than those of the PMN–PZT composites. It should be noted that some of the grains are observed to be in irregular shapes with some open pores. This is a result of a Pb-loss during the sintering process. Grains of the PMN ceramics are mostly in spherical-like shape, while grains of the secondary pyrochlore phase (Pb₂Nb₂O₇) exhibit a pyramidal morphology. Generally, the microstructures of PMN–PZT ceramic composites are seen as depending on compositions, and usually show mixed features of the two end-members. The grain size varies considerably from <1 to 7 μ m, as tabulated in table 1.

The experimental results of the uniaxial stress dependence of the dielectric properties of the ceramics in PMN-PZT

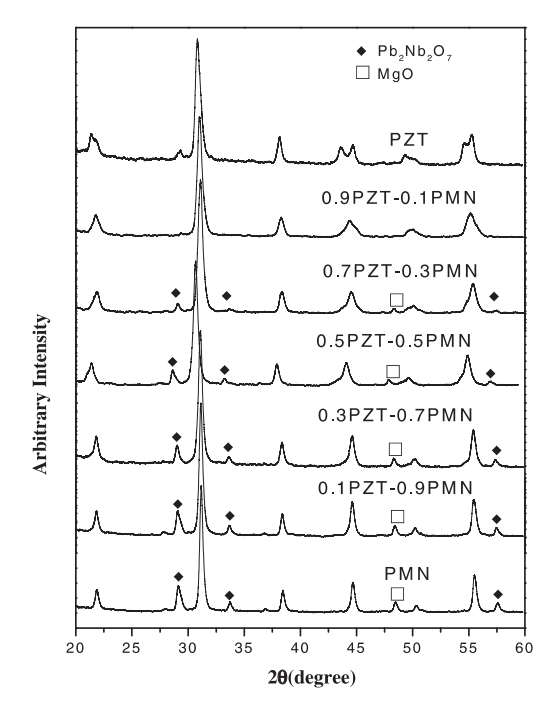


Figure 1. XRD patterns of the sintered (x)PMN–(1-x)PZT ceramics

system are shown in figures 3 and 4. There is a significant change of both the dielectric constant and the dielectric loss tangent of the ceramics when the applied stress increases from 0 to 5 MPa. The changes of the dielectric constant with the applied stress can be divided into two different groups. For PMN-rich compositions (PMN, 0.9PMN-0.1PZT, and 0.7PMN-0.3PZT), the dielectric constant generally decreases with increasing applied stress. However, it should be noticed that only PMN and 0.9PMN-0.1PZT compositions show definite decreases in the dielectric constant, while the dielectric constant of the 0.7PMN-0.3PZT composition initially increases then decreases with very little difference in the dielectric constant between applied stresses 0 and 5 MPa. On the other hand, for PZT-rich compositions (PZT, 0.1PMN-0.9PZT, 0.3PMN-0.7PZT, and 0.5PMN-0.5PZT), the dielectric constant rises slightly when the applied stress increases from 0 to 1 MPa, and becomes relatively constant when the applied stress increases further. The dielectric loss tangent for most compositions, except for PMN and PZT, is found to first increase when the applied stress is raised from 0 to 1 MPa, and then decrease with further increasing stress. However, for PZT ceramic the dielectric loss tangent increases monotonously with increasing stress, while PMN ceramic exhibits a slight increase in the dielectric loss tangent followed by a drop, the turning point being around 2 MPa.

To understand these experimental results, various effects have to be considered. Normally, the properties of ferroelectric materials are derived from both the intrinsic contribution, which is the response from a single domain, and extrinsic contributions, which are from domain wall motions [18, 19]. When a mechanical stress is applied to a ferroelectric material, the domain structure in the material will change to maintain the domain energy at a minimum; during this process some of the domains engulf other domains or change shape irreversibly. Under a uniaxial stress, the domain structure of ferroelectric ceramics may undergo domain switching, clamping of domain walls, de-aging, and de-poling [19].

In this study, the results for the case of PZT-rich compositions can easily be explained with the above statements. When the compressive uniaxial stress is applied in the direction parallel to the polar axis (poling) direction, the stress will move some of the polarization away from the poling direction resulting in a change in domain structures [18]. This change increases the non-180° domain wall density. Hence the increase of the dielectric constant is observed. The de-aging mechanism is also expected to play a role here. However, the stress clamping of domain walls and the de-poling mechanisms are not expected at this relative low stress level used in this study [12, 19, 20]. Therefore, a combination of the domain switching and the de-aging mechanisms is believed to be a reason for the slight increase of the dielectric constant with increasing applied stress in the PZT-rich compositions, as shown in figure 3. Since PMN is a relaxor ferroelectric material, the situation is very different for PMN-rich compositions. The stress dependence of the dielectric constant of the compositions is attributed to competing influences of the intrinsic contribution of non-polar matrix and the extrinsic contribution of re-polarization and growth of micro-polar regions [12,21]. Since the dielectric

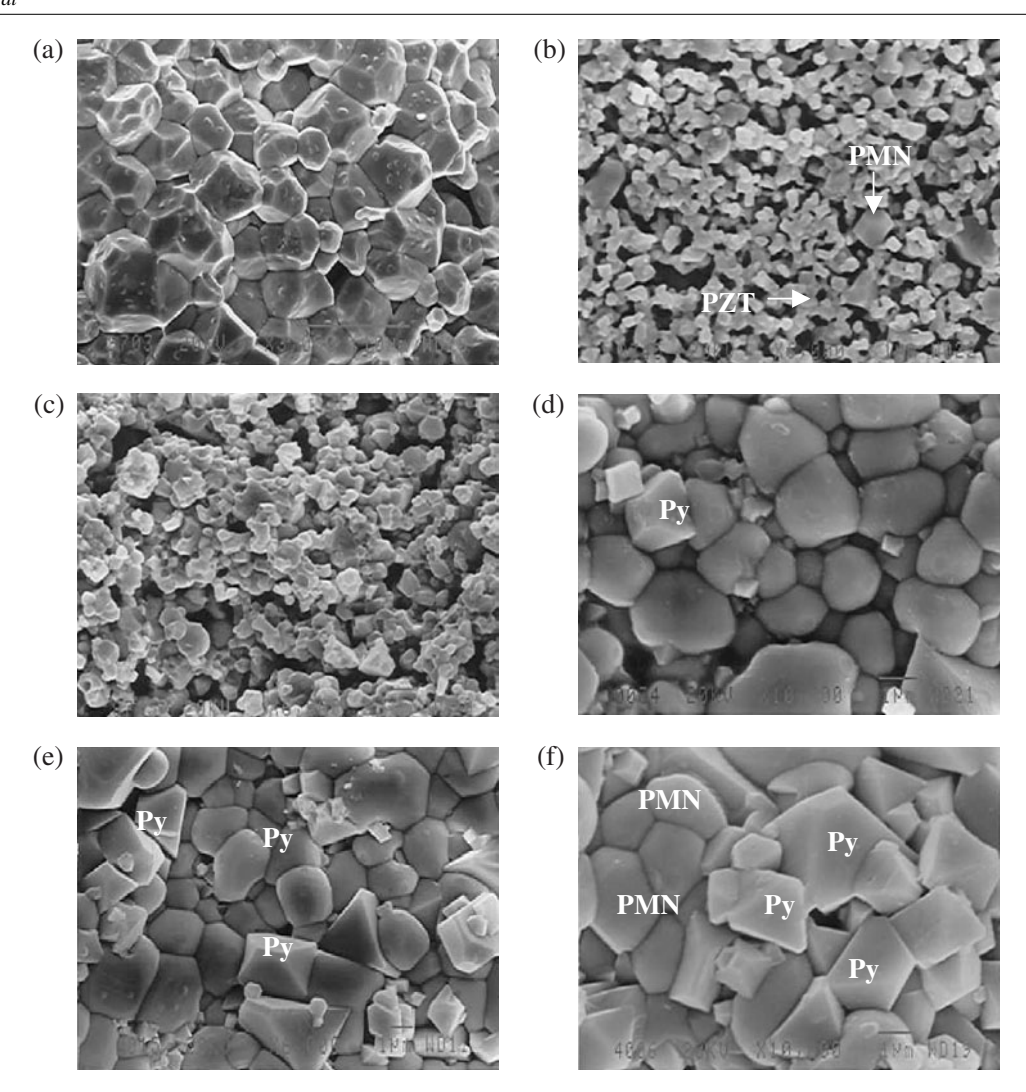


Figure 2. SEM micrographs of (x)PMN–(1-x)PZT ceramics sintered at 1150°C: (a) PZT, (b) 0.1PMN–0.9PZT, (c) 0.3PMN–0.7PZT, (d) 0.7PMN–0.3PZT, (e) 0.9PMN–0.1PZT, and (f) PMN (Py indicates pyrochlore phase).

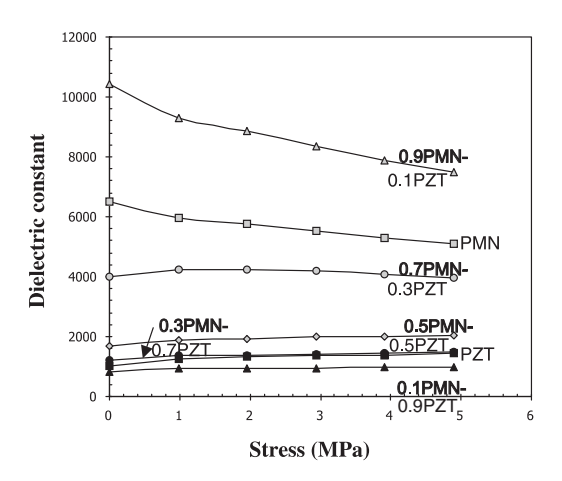
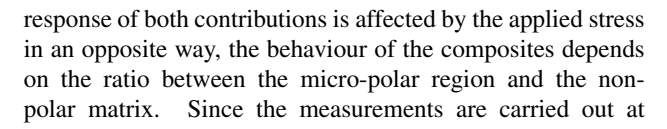


Figure 3. Uniaxial stress dependence of dielectric constant of PMN–PZT ceramics.



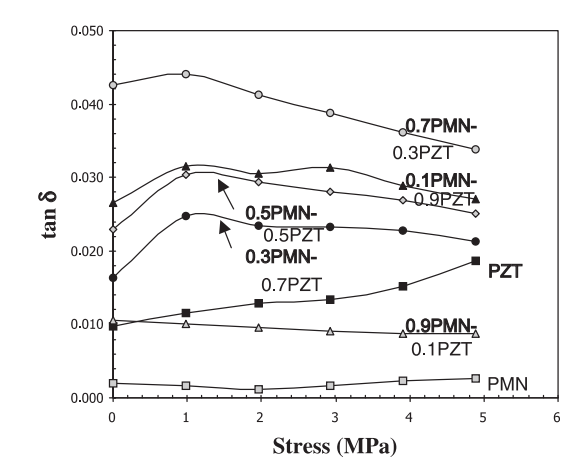


Figure 4. Uniaxial stress dependence of dielectric loss tangent of PMN–PZT ceramics.

the room temperature, the micro-polar regions dominate the dielectric response of the composites [21]. Therefore, the dielectric constant of the PMN-rich compositions decreases with increasing applied stress, as seen in figure 3.

The cause of the stress dependence of the dielectric loss tangent is a little more straightforward than that of the dielectric constant. As depicted in figure 4, an increase in domain wall mobility clearly enhances the dielectric loss tangent in some compositions, while the de-aging in the materials normally causes the decrease of the dielectric loss tangent observed in some compositions [19, 20].

These results clearly demonstrate that the contribution of each mechanism to the dielectric responses of the PMN–PZT ceramic depends on the compositions and the stress level.

4. Conclusions

this study. the (x)Pb $(Mg_{1/3}Nb_{2/3})O_3$ -(1-x) $Pb(Zr_{0.52}Ti_{0.48})O_3$ (when x = 0.0, 0.1, 0.3, 0.5, 0.7,0.9, and 1.0) ceramic composites are successfully prepared by a conventional mixed-oxide method at various processing conditions. The phase formation behaviour and the microstructure features are studied using the XRD and the SEM techniques, respectively. The measurements of physical properties reveal that the properties are relatively composition dependent. The dielectric properties under the uniaxial stress of the PMN-PZT ceramics are observed at stress levels up to 5 MPa using a calibrated uniaxial compressometer. The results clearly show that the dielectric constant of the PMN-rich compositions decreases, while that of the PZT-rich compositions increases slightly, with increasing applied stress. On the other hand, the dielectric loss tangent for most of the compositions first rises and then drops with increasing applied stress. This study undoubtedly shows that the applied stress has significant influences on the dielectric properties of the PMN-PZT ceramic composites.

Acknowledgment

This work is supported by the Thailand Research Fund (TRF).

References

- [1] Cross L E 1987 Ferroelectrics 76 241
- [2] Xu Y H 1991 Ferroelectric Materials and their Applications (Los Angeles: North-Holland)
- [3] Viehland D and Powers J 2001 J. Appl. Phys. 89 1820
- [4] Ouchi H, Nagano K and Hayakawa S J 1965 J. Am. Ceram. Soc. 48 630
- [5] Ouchi H 1968 J. Am. Ceram. Soc. 51 169
- [6] Abe Y, Yanagisawa Y, Kakagawa K and Sasaki Y 2000 Solid State Commun. 113 331
- [7] Murty K V R, Murty S N, Mouli K C and Bhanumathi A 1992 Proc. IEEE International Symp. on Applications of Ferroelectrics p 144
- [8] Yoo J H, Yoon H S, Jeong Y H and Park C Y 1998 Proc. IEEE Ultrasonic Symp. p 981
- [9] Shilnikov A V, Sopit A V, Burkhanov A I and Luchaninov A G 1999 J. Euro. Ceram. Soc. 19 1295
- [10] He L X, Gao M, Li C E, Zhu W M and Yan H X 2001 J. Euro. Ceram. Soc. 21 703
- [11] Stringfellow S B, Gupta S, Shaw C, Alcock J R and Whatmore R W 2002 J. Euro. Ceram. Soc. 22 573
- [12] Zhao J and Zhang Q M 1996 Proc. IEEE International Symp. on Applications of Ferroelectrics p 971
- [13] Zhao J, Glazounov A E and Zhang Q M 1999 Appl. Phys. Lett. 74 436
- [14] Swartz S L and Shrout T R 1982 Mater. Res. Bull. 17 1245
- [15] Yimnirun R 2001 *PhD Thesis* The Pennsylvania State University
- [16] Koval V, Alemany C, Briancin J, Brunckova H and Saksl K 2003 J. Euro. Ceram. Soc. 23 1157
- [17] Park J H, Yoon K H and Kang D H 2001 *Thin Solid Films* 396 84
- [18] Zhang Q M, Zhao J, Uchino K and Zheng J 1997 J. Mater. Res. 12 226
- [19] Yang G, Liu S F, Ren W and Mukherjee B K 2000 Proc. SPIE Symp. on Smart Structures and Materials vol 3992, p. 103
- [20] Yang G, Ren W, Liu S F, Masys A J and Mukherjee B K 2000 Proc. IEEE Ultrasonic Symp. p 1005
- [21] Zhao J, Zhang Q M and Mueller V 1998 Proc. IEEE
 International Symp. on Applications of Ferroelectrics
 p 361



Materials Science & Engineering B 112 (2004) 79-86



www.elsevier.com/locate/mseb

Effects of Pb(Mg_{1/3}Nb_{2/3})O₃ mixed-oxide modification on dielectric properties of Pb(Zr_{0.52}Ti_{0.48})O₃ ceramics

Rattikorn Yimnirun^{a,*}, Supon Ananta^a, Pitak Laoratanakul^b

^aDepartment of Physics, Faculty of Science, Chiang Mai University, Chiang Mai 50200, Thailand ^bNational Metal and Materials Technology Center, Pathumtani 12120, Thailand

Received 22 March 2004; accepted 12 June 2004

Abstract

The dielectric properties of (1-x)Pb($Zr_{0.52}Ti_{0.48}$)O₃–(x)Pb($Mg_{1/3}Nb_{2/3}$)O₃ (when x=0,0.1,0.3,0.5,0.7,0.9, and 1.0) ceramics prepared by an oxide-mixing method are determined by means of an automated dielectric measurement set-up. The dielectric constant and dielectric loss tangent of the ceramics are measured as functions of both temperature and frequency. The results indicate that the dielectric properties of the pure phase PZT and PMN are of normal and relaxor ferroelectric behaviors, respectively. The dielectric behaviors of the 0.9PZT–0.1PMN and 0.7PZT–0.3PMN ceramics are more of normal ferroelectrics, while the other compositions are obviously of relaxor ferroelectrics. However, with a higher degree of disorder the PMN-modified PZT shows more diffuse phase transition nature than the pure PMN. In addition, the transition temperature decreases and the maximum dielectric constant increases with increasing PMN content in the system. The rate of transition temperature change, however, depends significantly on the Zr/Ti ratio of PZT.

Keywords: PMN-PZT; Mixed-oxide; Dielectric properties

1. Introduction

Among the lead-based complex perovskites, lead zirconate titanate (Pb(Zr_{1-x}Ti_x)O₃ or PZT) and lead magnesium niobate (Pb(Mg_{1/3}Nb_{2/3})O₃ or PMN) ceramics have been investigated extensively, both from academics and commercial viewpoints [1-3]. With the complementary features of PZT and PMN described in many publications [4–10], the solid solutions between PZT and PMN are expected to combine the properties of both normal ferroelectric PZT and relaxor ferroelectric PMN, which could exhibit better piezoelectric and dielectric properties than those of the single-phase PZT and PMN. Furthermore, the properties can also be tailored over a wider range by changing the compositions to meet the strict requirements for specific applications [9–11]. Recently, there have been several investigations on PMN-PZT system [4-10,12-14]. Many of these works have been on the PMNZT system, in which the starting oxide precursors are mixed together to form stoichiometric compositions of Pb(Zr_xTi_{1-x})_{0.8}(Mg_{1/3}Nb_{2/3})_{0.2}-O₃ (where x =0.43-0.49) [13], and the ternary system of xPb(Mg_{1/3}Nb_{2/3})- O_3 -yPbTi O_3 -zPbZr O_3 (x + y + z = 1) [4,5,15]. Thus far, these previous works have only been focused on a few compositions in the vicinity of the morphotropic phase boundary (MPB) such as $0.125Pb(Mg_{1/3}Nb_{2/3})O_3-0.435PbTiO_3-0.44PbZrO_3$ and $0.5Pb(Mg_{1/3}Nb_{2/3})O_3-0.375PbTiO_3-0.125PbZrO_3$ [1,8,12] and of the end members such as 0.11Pb(Zr_{0.53}Ti_{0.47})O₃- $0.89Pb(Mg_{1/3}Nb_{2/3})O_3$ and $0.82Pb(Zr_{0.52}Ti_{0.48})O_3-0.18Pb$ $(Mg_{1/3}Nb_{2/3})O_3$ [9,10,14, 16,17]. However, there has been no systematic study on dielectric properties of the ceramics within the entire compositional range between PMN and PZT at MPB composition, e.g. Pb(Zr_{0.52}Ti_{0.48})O₃. Therefore, as an extension to the research on the PMN-PZT ceramics, the overall purpose of this study is to determine the temperature and frequency dependence of the dielectric properties of ceramics in the $(1 - x)Pb(Zr_{0.52}Ti_{0.48})O_3-(x)Pb$ $(Mg_{1/3}Nb_{2/3})O_3$ (when x = 0, 0.1, 0.3, 0.5, 0.7, 0.9, and 1)binary system prepared by a conventional mixed-oxide method.

^{*} Corresponding author. Tel.: +66 53 943376; fax: +66 53 357512 *E-mail address:* rattikor@chiangmai.ac.th (R. Yimnirun).

2. Experimental

The PMN-PZT ceramics used in this study are prepared from PMN and PZT starting powders with a conventional mixed-oxide method. Initially, perovskite-phase PMN powders are obtained via a well-known columbite method, while PZT powders are prepared by the mixed-oxide method. With the columbite method, the magnesium niobate powders are first prepared by mixing starting MgO (>98%) and Nb₂O₅ (99.9%) powders and then calcining the mixed powders at 1050 °C for 2.5 h. This yields a so-called columbite powder (MgNb₂O₆). The columbite powders are subsequently ball-milled with PbO (99%) for 24 h. The mixed powders are calcined at 800 °C for 2.5 h to form a perovskite-phase PMN. With a conventional oxide-mixing route, PZT powders are prepared from reagent-grade PbO (99%), ZrO₂ (99%), and TiO₂ (98.5%) starting powders. These powders are ball-milled for 24 h and later calcined at 850 °C for 2 h. Subsequently, the $(1 - x)Pb(Zr_{0.52}Ti_{0.48})O_{3}-(x)Pb(Mg_{1/3}Nb_{2/3})O_{3}$ (when x =0, 0.1, 0.3, 0.5, 0.7, 0.9, and 1.0) ceramic composites are prepared from the PZT and PMN powders by the mixedoxide method at various processing conditions. For optimization purpose, the sintering temperature is varied between 1000 and 1300 °C depending upon the compositions [6]. The physical characteristics of the ceramics are then determined with the following procedures. The densities of the sintered ceramics are measured by Archimedes method. The phase formations of the sintered specimens are studied by an X-ray diffractometer (Philips Analytical). The microstructure analyses are undertaken by a scanning electron microscopy (SEM: JEOL Model JSM 840A). Grain size is determined from SEM micrographs by a linear intercept method.

For electrical properties characterizations, the sintered samples are lapped to obtain parallel faces, and the faces are then coated with silver paint as electrodes. The samples are heat-treated at 750 °C for 12 min to ensure the contact between the electrodes and the ceramic surfaces. The dielectric properties of the sintered ceramics are studied as functions of both temperature and frequency with an automated dielectric measurement system. The computer-controlled dielectric measurement system consists of a precision LCR-meter (Hewlett Packard, model 4284A), a temperature chamber (Delta Design, model 9023), and a computer system. The capacitance and the dielectric loss tangent are determined over the temperature range of -150 and 400 °C with the frequency ranging from 100 Hz to 1 MHz. The measurements are carried out on cooling continuously. Before each cooling run, the samples are first heated up to 400 °C and then cooling run is performed at the rate of 3 °C/min. The dielectric constant is then calculated from $\varepsilon_{\rm r} = Cd/\varepsilon_0 A$, where C is the capacitance of the sample, d and A are the thickness and the area of the electrode, respectively, and ε_0 is the dielectric permittivity of vacuum $(8.854 \times 10^{-12} \text{ F/m}).$

3. Experimental results

3.1. Physical properties

Fig. 1 shows the phase formation behavior of the sintered ceramics. The XRD patterns indicate that the sintered ceramics are mainly in perovskite phase with small impurity inclusions. From the XRD pattern, PZT ceramic is identified as a single-phase material with a perovskite structure having tetragonal symmetry, while PMN ceramic is a perovskite material with a cubic symmetry [8]. All PMN-PZT ceramic composites exhibit pseudocubic crystal structure, as reported in previous investigations [4,5,13]. However, some impurity phases (Pb₂Nb₂O₇ and MgO) are also detected on the XRD patterns of the composites with x > 0.1. The secondary pyrochlore phase (Pb₂Nb₂O₇) is clearly present on the SEM micrographs as cubic particles, resulting in very heterogeneous microstructure (Fig. 2(c-d)). The optimized density of sintered (1 - x)PZT-(x)PMN ceramics is listed in Table 1. The density of the ceramic compositions with x =0.1 and 0.3 is 6.09 and 7.45, in the units of g/cm³, respectively, which is relatively lower than that of the other compositions (varied between 7.59 and 7.90, in the units of g/cm³). The SEM investigations (Fig. 2) reveal supporting evidence that the ceramics with these two compositions contain very small and loosely bonded grains. It should,

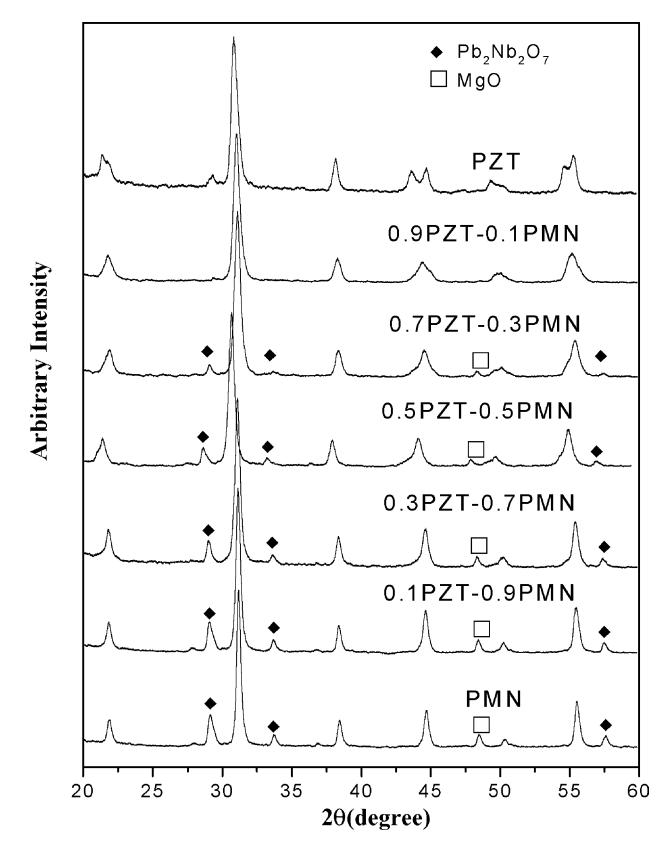


Fig. 1. XRD diffraction patterns of the sintered (1 - x)PZT-(x)PMN ceramics.

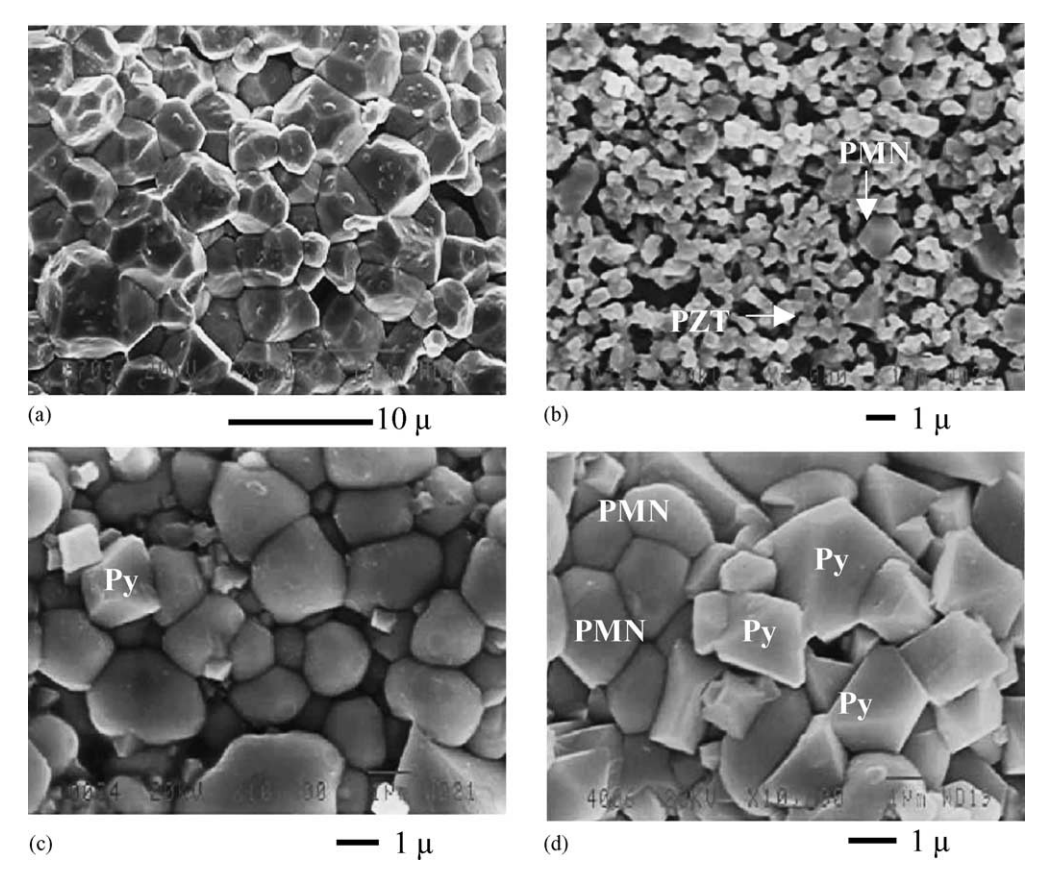


Fig. 2. SEM micrographs of (1 - x)PZT-(x)PMN ceramics sintered at 1150 °C: (a) PZT; (b) 0.9PZT-0.1PMN; (c) 0.3PZT-0.7PMN; and (d) PMN (Py indicates pyrochlore phase).

however, be noted that the composition with x = 0.1, which contains sub-micron size grains, is not well sintered. Clearly, this is a reason for the much lower density in this composition. As shown in Table 1, the average grain size of all the mixed compositions is much smaller than that of the pure PZT and PMN materials. The grain size varies considerably from <1 to 7 μ m. The reason for the changes of the density and the smaller grain sizes in the mixed compositions is not clearly understood, but this may be a result of PMN's role as a grain-growth inhibitor in the PMN–PZT composites, as described in the earlier work by Koval et al. [8]. In that study, it was found that the PMN modification reduced the rate of grain growth in xPMN–(1 - x)PZT ceramics. The average grain size decreased from 2.2 μ m for x = 0.125 to approximately 1 μ m for the compositions with x = 0.5 [8]. In the

present study, the average grain size decreases from 5.23 μ m in PZT to <2 μ m in PMN–PZT compositions. More importantly, it should be pointed out that dense ceramics for PMN–PZT composites are very difficult to obtain as a result of a narrow range of sintering behavior of PMN material, in which a perovskite-type structure is formed between 850 and 950 °C whilst a pyrochlore structure is formed between 750 and 850 °C [4]. This is particular critical in ceramics with high PMN content, which show very heterogeneous microstructure as a result of the secondary pyrochlore phase. This could very well be a limit of the mixed-oxide method at high PMN content, even when used in conjunction with a columbite-precursor method. As a result, many investigators have alternatively prepared better PMN–PZT ceramics by carefully controlling the Zr/Ti ratio [8–10], by using a

Table 1 Characteristics of PMN-PZT ceramics with optimized processing conditions

Ceramic	Density (g/cm ³)	Grain size range (µm)	Average grain size (µm)	
PZT	7.59 ± 0.11	2–7	5.23	
0.9PZT-0.1PMN	6.09 ± 0.11	0.5–2	0.80	
0.7PZT-0.3PMN	7.45 ± 0.10	0.5–3	1.65	
0.5PZT-0.5PMN	7.86 ± 0.05	0.5–5	1.90	
0.3PZT-0.7PMN	7.87 ± 0.07	1–4	1.40	
0.1PZT-0.9PMN	7.90 ± 0.09	1–4	1.50	
PMN	7.82 ± 0.06	2–4	3.25	

combination of wet–dry methods, or by doping with other elements [4,5,12,14].

3.2. Dielectric properties

The dielectric properties, e.g. dielectric constant (ε_r) and tan δ , of the (1 - x)PZT-(x)PMN are measured as functions

of both temperature and frequency, as shown in Fig. 3(a–d). Except for PZT, the maximum dielectric constant increases steadily with increasing PMN content (ε_r increases from \sim 3700 in 0.9PZT–0.1PMN to \sim 10700 in 0.1PZT–0.9PMN), as listed in Table 2. The PMN is expected to show larger value of the dielectric constant, but the lower value is attributed to the detrimental effect of the secondary pyrochlore

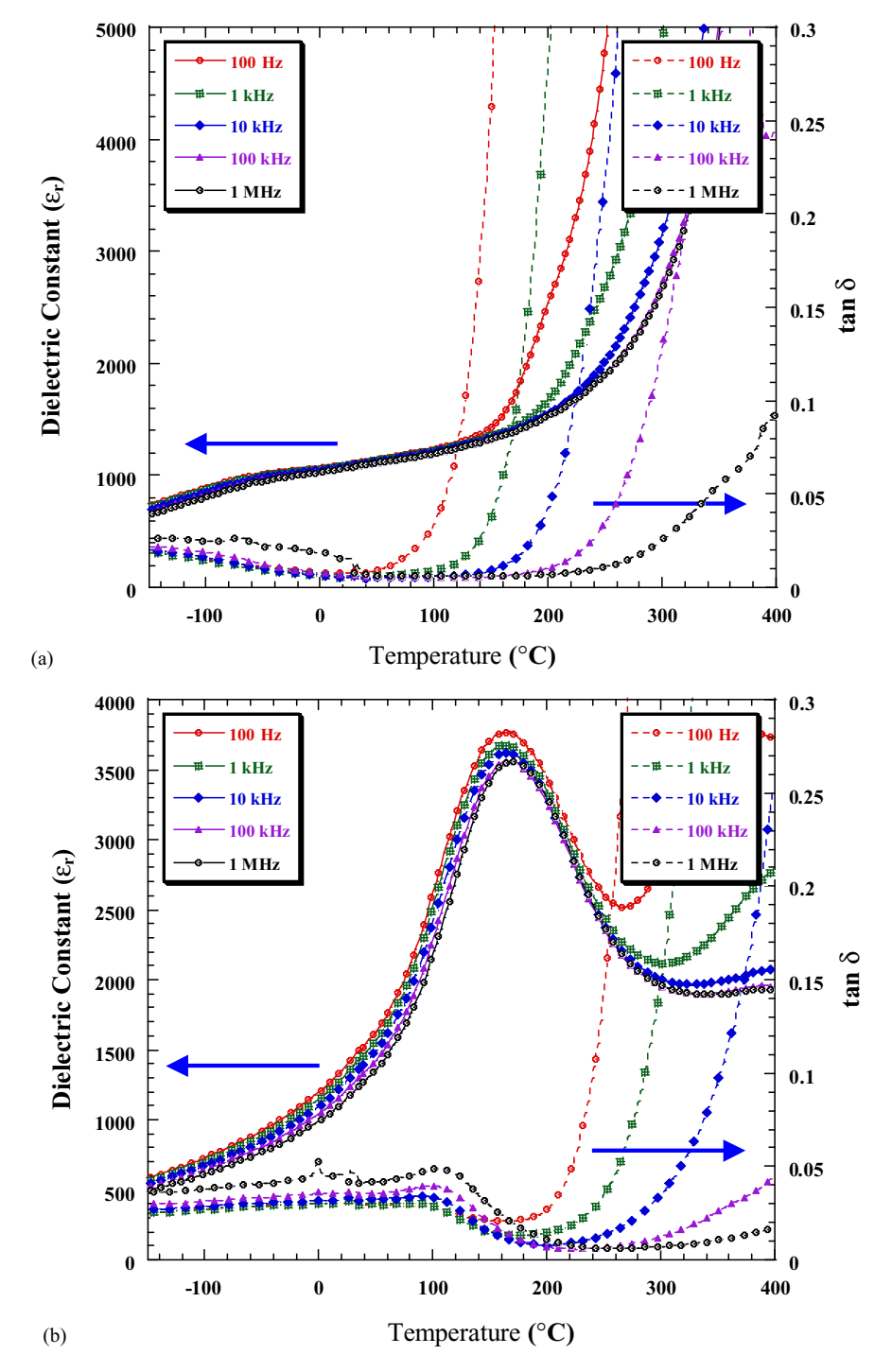
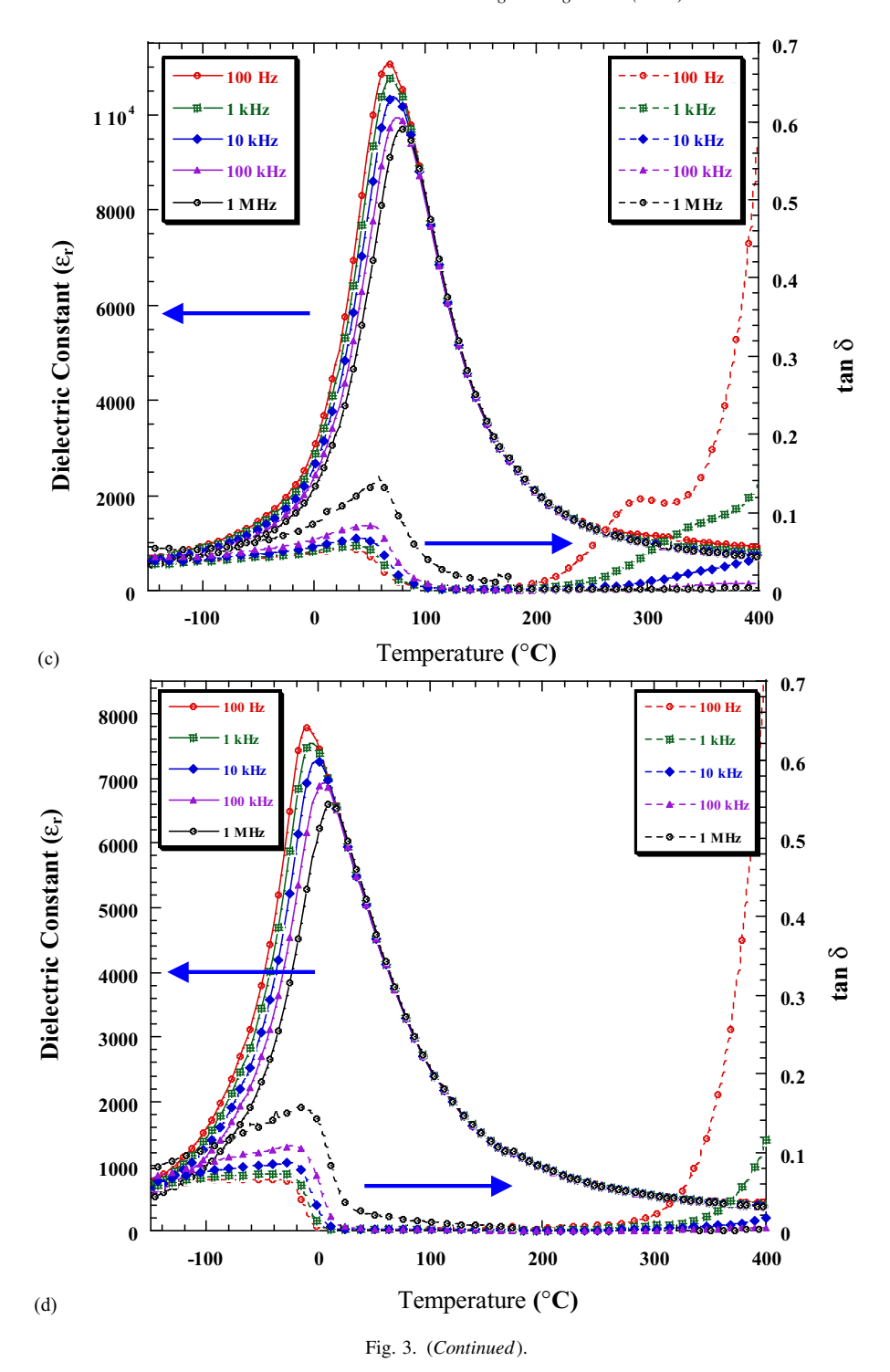


Fig. 3. (a) Temperature and frequency dependences of dielectric properties of PZT ceramic. (b) Temperature and frequency dependences of dielectric properties of 0.7PZT-0.3PMN ceramic. (c) Temperature and frequency dependences of dielectric properties of 0.3PZT-0.7PMN ceramic. (d) Temperature and frequency dependences of dielectric properties of PMN ceramic.



phase [16]. The dielectric properties of PZT ceramic, as plotted in Fig. 3(a), change significantly with temperature, but are nearly independent of frequency, except in the vicinity of the phase transformation temperature. This is a typical characteristic of ferroelectric ceramics with a long-range ordered structure [1,8]. The Curie temperature ($T_{\rm C}$) for PZT ceramic is not determined in this study as a result of limited range of the measuring set-up, though is widely known to be close to 400 °C [2,3,11,18]. While PZT exhibits

a normal ferroelectric behavior, PMN is a well-known relaxor ferroelectric material as a result of a short-range ordered structure with a nanometer scale heterogeneity in composition [8]. In typical relaxor ferroelectrics [3,11], both dielectric constant (ε_r) and dielectric loss tangent (tan δ) exhibit strong temperature–frequency dependence below the transition temperature, as shown in Fig. 3(d) for PMN ceramic. In this case, the temperatures of maximum dielectric constant and dielectric loss tangent are shifted to higher

Table 2 Dielectric properties of xPMN–(1 - x)PZT ceramics (at 1 kHz)

Ceramic	T _C (°C)	Dielectric prop	Dielectric properties (at T_{Max})		roperties (at 25 °C)	Diffusivity (γ) (at 1 kHz)
		$\varepsilon_{ m r}$	tan δ	$\varepsilon_{\rm r}$	tan δ	
PZT	_	>29,000	0.010	1,100	0.006	_
0.9PZT-0.1PMN	_	$\sim 3,700$	0.020	700	0.020	_
0.7PZT-0.3PMN	160	3,800	0.030	1,400	0.030	1.62
0.5PZT-0.5PMN	115	6,100	0.045	2,200	0.040	1.83
0.3PZT-0.7PMN	71	10,100	0.057	5,600	0.057	1.80
0.1PZT-0.9PMN	16	10,700	0.077	10,300	0.001	1.56
PMN	-8	7,600	0.073	6,000	0.001	1.49

temperature with increasing frequency. The maximum value of the dielectric constant decreases with increasing frequency, while that of the dielectric loss tangent increases. The dielectric properties then become frequency independent above the transition temperature [1,8].

The effect of PMN modification on the dielectric properties of PZT is then investigated. When PMN is added to form the binary system with PZT, the dielectric behavior is shifted towards that of relaxor materials, in which the dielectric properties vary significantly with frequency below the phase transition temperature. The results shown in Fig. 3(a–d) clearly indicate such a trend. However, with relatively small amount of PMN added, such as in 0.9PZT–0.1PMN and 0.7PZT–0.3PMN ceramics, the dielectric properties exhibit a mixture of both normal and relaxor characteristics, for instance as shown in Fig. 3(b) in which the transition temperature is not shifted as much as for other relaxor-like

ceramics. Similar tendency has also been observed in several prior investigations [1,4,8]. It should also be noted here that the dielectric properties in all ceramics increase significantly at high temperature as a result of thermally activated space charge conduction.

To assess the transition from the normal ferroelectric behavior to the relaxor one, the degree of broadening or diffuseness in the observed dielectric variation could be estimated with the diffusivity (γ) using the expression $\ln(1/\varepsilon_{\rm r}-1/\varepsilon_{\rm max})$ versus $(T-T_{\rm max})^{\gamma}$. The value of γ can vary from (1) for normal ferroelectrics with a normal Curie–Weiss behavior, to (2) for completely disordered relaxor ferroelectrics [19–21]. The relation between $(1/\varepsilon_{\rm r}-1/\varepsilon_{\rm max})$ and $(T-T_{\rm max})$ can be plotted on a log-log graph for each composition and the slope of the graph represents the exponent γ for the composition. The plots shown in Fig. 4 shows that the variation for each composition is very

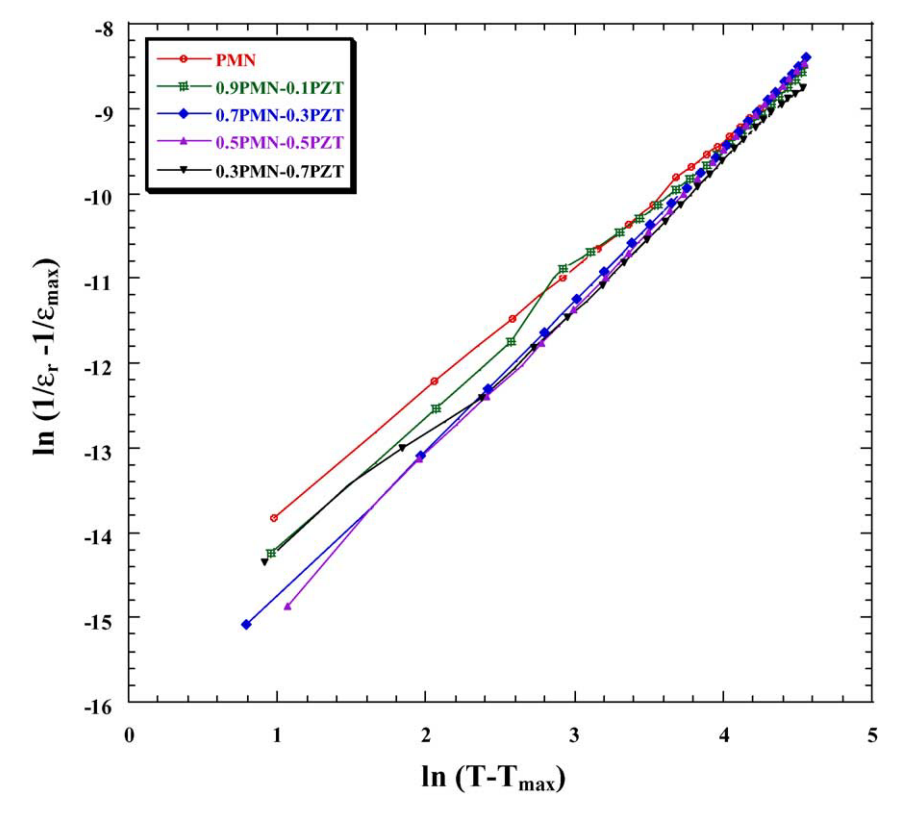


Fig. 4. Variation of $\ln(1/\epsilon_r - 1/\epsilon_{max})$ vs. $\ln(T - T_{max})$ of (1 - x)PZT - (x)PMN ceramics in the paraelectric region at 1 kHz.

linear. The mean value of the diffusivity (γ) for each composition is extracted from these plots by fitting a linear equation. The values of γ listed in Table 2 vary between 1.49 and 1.83, which confirms that diffuse phase transitions occur in PMN-PZT ceramics with a high degree of disorder. It is expected that PMN should have the highest degree of disorder, but the calculation somewhat indicates that addition of PMN into PZT leads to lower degree of disorder (the value of γ decreases from 1.83 for 0.5PZT-0.5PMN to 1.49 for PMN). Since for a perovskite ferroelectric it is established that the diffuseness could be also caused by the decrease of grain size [1], the observed difference of the degree of the diffuseness could be a result of the grain size variation. Therefore, this effect can partly be the cause of the increase of the diffusivity when PZT is added to PMN since the average grain size decreases from 3.25 µm in PMN to 1.90 µm in 0.5PZT-0.5PMN. Additionally, the reason for the observation could also be attributed to a formation of secondary pyrochlore phase in high PMN-content composi-

Furthermore, as shown in Table 2 since the transition temperature of PMN is very low (-8 °C at 1 kHz) and its maximum dielectric constant is very high (\sim 7600 at 1 kHz), it is also expected to observe that the transition temperature decreases and the maximum dielectric constant increases with increasing amount of PMN in the system [8]. This is clearly evident in Fig. 5. Fig. 6 shows that the transition temperature (at 1 kHz for this case) moves towards lower temperature almost linearly with the average rate of \sim 2.4 °C/mol% as the molar fraction of PMN in the composition increases. However, it is noted that this relationship does not cover the compositions 0.9PZT-0.1PMN and pure-phase PZT, which are expected to have the transition temperature near 400 °C, shown in Fig. 6 as open circles. The reason is not clearly known, but could be attributed to the pseudo-binary nature of this system, as described in the earlier publication [6], in which PZT and

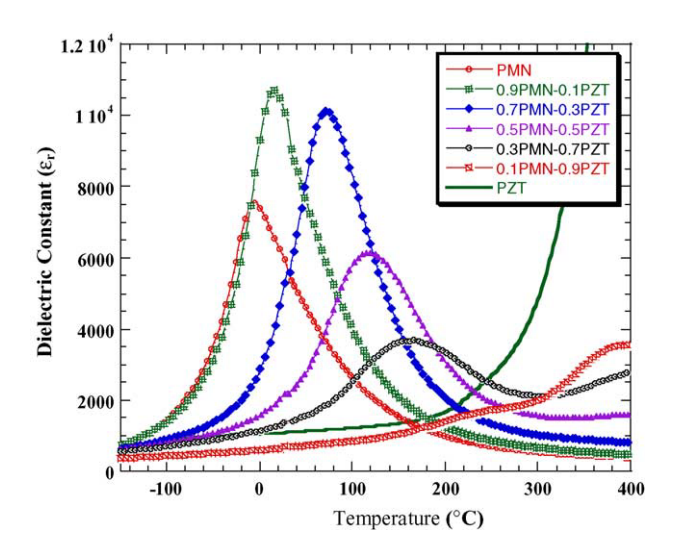


Fig. 5. Temperature dependence of dielectric constant of (1 - x)PZT-(x)PMN ceramics (measured at 1 kHz).

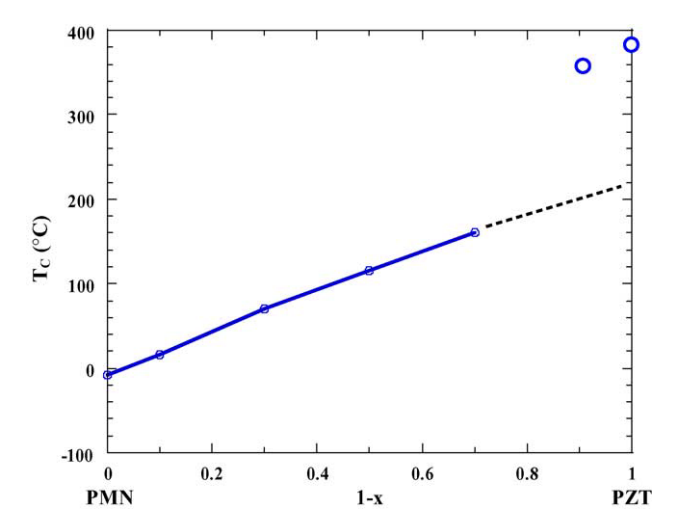


Fig. 6. Curie temperature of (1 - x)PZT-(x)PMN ceramics (measured at 1 kHz).

PMN do not form a complete solid solution, but rather a composite. Moreover, it could also be a discontinuity at the composition of the morphotropic phase boundary, as previously described in literatures [1,4,5]. It is very of interest to see that a previous investigation by Koval et al. [1] reported that the transition temperature of PMN–PZT system moved towards lower temperature with the rate of –4.1 °C/mol% of PMN in the composition. The difference is believed to be the influence of the Zr/Ti ratio in PZT because in the work by Koval et al. the Zr/Ti ratio is 47/53 while in our study the ratio is 52/48.

4. Conclusions

The (1-x)Pb $(Zr_{0.52}Ti_{0.48})O_3-(x)$ Pb $(Mg_{1/3}Nb_{2/3})O_3$ (when x = 0, 0.1, 0.3, 0.5, 0.7, 0.9, and 1.0) ceramic composites are prepared from PZT and PMN powders by a mixed-oxide method. The dielectric properties of the ceramics are determined as functions of both temperature and frequency with an automated dielectric measurement system. The dielectric measurement takes place over the temperature range of -150 and 400 °C with measuring frequency between 100 Hz and 1 MHz. The results indicate that the dielectric properties of the pure phase PZT and PMN follow that of normal and relaxor ferroelectric behaviors, respectively. The dielectric behaviors of the 0.9PZT-0.1PMN and 0.7PZT-0.3PMN ceramics are more of normal ferroelectrics, while the other compositions are obviously of relaxor ferroelectrics. However, it is very interesting to see that the addition of PMN into PZT leads to lower degree of disorder, even though PMN should show the highest degree of disorder. It is also observed that the transition temperature decreases and the maximum dielectric constant increases with increasing amount of PMN in the system. The rate of transition temperature change, however, depends significantly on the Zr/Ti ratio of PZT.

Acknowledgment

The authors would like to express their gratitude for financial support from the Thailand Research Fund (TRF).

References

- V. Koval, C. Alemany, J. Briancin, H. Brunckova, J. Electroceram. 10 (2003) 19.
- [2] G.H. Haertling, J. Am. Ceram. Soc. 82 (1999) 797.
- [3] L.E. Cross, Mater. Chem. Phys. 43 (1996) 108.
- [4] H. Ouchi, K. Nagano, S.J. Hayakawa, J. Am. Ceram. Soc. 48 (1965) 630.
- [5] H. Ouchi, J. Am. Ceram. Soc. 51 (1968) 169.
- [6] R. Yimnirun, S. Ananta, E. Meechoowas, S. Wongsaenmai, J. Phys. D: Appl. Phys. 36 (2003) 1615.
- [7] L.X. He, M. Gao, C.E. Li, W.M. Zhu, H.X. Yan, J. Euro. Ceram. Soc. 21 (2001) 703.
- [8] V. Koval, C. Alemany, J. Briancin, H. Brunckova, K. Saksl, J. Euro. Ceram. Soc. 23 (2003) 1157.

- [9] A.V. Shilnikov, A.V. Sopit, A.I. Burkhanov, A.G. Luchaninov, J. Euro. Ceram. Soc. 19 (1999) 1295.
- [10] A.I. Burkhanov, A.V. Shilnikov, A.V. Sopit, A.G. Luchaninov, Phys. Solid State 42 (2000) 936.
- [11] L.E. Cross, Ferroelectrics 76 (1987) 241.
- [12] J.C. Shaw, K.S. Lin, I.N. Lin, Scripta Mater. 29 (1993) 981.
- [13] Y. Abe, Y. Yanagisawa, K. Kakagawa, Y. Sasaki, Solid State Commun. 113 (2000) 331.
- [14] S.B. Stringfellow, S. Gupta, C. Shaw, J.R. Alcock, R.W. Whatmore, J. Euro. Ceram. Soc. 22 (2002) 573.
- [15] R.W. Whatmore, O. Molter, C.P. Shaw, J. Euro Ceram. Soc. 23 (2003) 721
- [16] C.H. Wang, J. Euro. Ceram. Soc. 22 (2002) 2033.
- [17] J.H. Park, K.H. Yoon, D.H. Kang, Thin Solid Films 396 (2001) 84.
- [18] W.C. Las, P.D. Spagnol, M.A. Zaghete, M. Cilense, Ceram. Int. 27 (2001) 367.
- [19] S.R. Shannigrahi, F.E.H. Tay, K. Yao, R.N.P. Choudhary, J. Euro. Ceram. Soc. 24 (2004) 163.
- [20] R. Rai, S. Sharma, Solid State Commun. 129 (2004) 305.
- [21] E.F. Alberta, A.S. Bhalla, J. Phys. Chem. Solids 63 (2002) 1759.

Change of dielectric properties of ceramics in lead magnesium niobate-lead titanate system with compressive stress

Rattikorn Yimnirun, Muangjai Unruan, Yongyut Laosiritaworn and Supon Ananta

Department of Physics, Faculty of Science, Chiang Mai University, Chiang Mai 50200, Thailand

Received 27 February 2006, in final form 12 June 2006 Published 30 June 2006 Online at stacks.iop.org/JPhysD/39/3097

Abstract

Effects of compressive stress on the dielectric properties of PMN–PT ceramics were investigated. The ceramics with the formula (1-x)Pb $(Mg_{1/3}Nb_{2/3})O_3$ -(x)PbTiO₃ or (1-x)PMN-(x)PT (x=0.1-0.5) were prepared by a conventional mixed-oxide method and then characterized with x-ray diffraction (XRD) and scanning electron microscopy. Dense perovskite-phase PMN-PT ceramics with uniform microstructure were successfully obtained. The dielectric properties under compressive stress were observed at stress up to 230 MPa using a home-built compressometer. The experimental results revealed that the superimposed compression stress significantly reduced both the dielectric constant and the dielectric loss tangent of 0.9PMN-0.1PT ceramic, while the changes were not as significant in the other PMN-PT ceramic compositions. In addition, the dielectric properties were considerably lowered after a stress cycle. Since change in the dielectric properties with applied stress was attributed to the competing influences of the intrinsic and the extrinsic contributions, the observations were mainly interpreted in terms of domain switching through non-180° domain walls, de-ageing, clamping of domain walls and the stress induced decrease in the switchable part of spontaneous polarization.

(Some figures in this article are in colour only in the electronic version)

1. Introduction

A family of materials which are of great interest due to their high polarizabilities is the lead-based relaxor ferroelectrics, particularly lead magnesium niobate, $Pb(Mg_{1/3}Nb_{2/3})O_3$ (PMN) and its solid solution with lead titanate, $PbTiO_3$ (PT), the so-called PMN–PT. These compounds have dielectric constants in excess of 20 000, making them potential candidates for capacitive applications. In addition, they also exhibit electrostrictive behaviour at temperatures above their phase transition temperatures. This behaviour extends their use to transducer and actuator applications [1–5]. $(1-x)Pb(Mg_{1/3}Nb_{2/3})O_3$ - $(x)PbTiO_3$ or (1-x)PMN-(x)PT ceramic compositions with x < 0.2 have been studied for electrostrictive applications [4–7], while those with x > 0.2 can be utilized as piezoelectric materials [4, 6, 8, 9].

The differences between the electrostrictive and piezoelectric compositions of PMN–PT are due to differences in the degree of long-range polar order [4,7,10]. In the compositions with lower PT content, relaxor ferrfoelectric characteristics with polar clusters or nanodomains are observed [4,11,12]. On the other hand, long-range polar order with normal micrometresized ferroelectric domains exists in the compositions with higher PT content [4,9,10].

Practically, when used in specific applications PMN-PT ceramics are often subjected to mechanical loading, either deliberately in the design of the device itself or because the device is used to change shapes as in many smart structure applications or the device is used under environmental stresses [8, 13–17]. A prior knowledge of how the material properties change under different load conditions is crucial for the proper design of a device and for suitable selection of

materials for a specific application. Despite this fact, material constants used in any design calculations are often obtained from a stress-free measuring condition, which in turn may lead to incorrect or inappropriate actuator and transducer designs. It is therefore important to determine the properties of these materials as a function of applied stress. Previous investigations on the stress-dependence electrical properties of many ceramic systems have clearly emphasized the importance of this matter [7, 15, 18–23]. Recently, the uniaxial stress dependence of dielectric properties has been investigated in materials such as BT, PZT, PMN and PMN-PZT [19-22]. The results clearly showed that the effects of stress on the dielectric properties depended significantly on ceramic compositions and stress levels. Since PMN-PT ceramics are practically very important, there have been previous reports on the electromechanical properties of electrostrictive 0.9PMN-0.1PT and piezoelectric 0.7PMN-0.3PT ceramics under various mechanical and electrical loading conditions [7,15,23,24]. However, there has been no systematic study on the influence of an applied stress on the dielectric properties of ceramics in the PMN-PT system. Therefore, it is the aim of this study to determine the dielectric properties of the (1-x)PMN– (x)PT ceramics as a function of compressive stress.

2. Experimental method

PMN–PT ceramics were prepared from starting PMN and PT powders by a conventional mixed-oxide method. Perovskite-phase PMN powders were obtained from the columbite method, while PT powders were prepared by a simple mixed-oxide method [25]. To obtain the perovskite-phase PMN, the magnesium niobate powders were first prepared by mixing MgO (99.0%) and Nb₂O₅ (99.9%) powders and then calcining the mixed powders at $1100\,^{\circ}\text{C}$ for 3 h, to yield so called columbite powders (MgNb₂O₆). After that, the columbite powders were mixed with PbO (99.9%) by the ball-milling method and calcined at $800\,^{\circ}\text{C}$ for 1 h to form the perovskite-phase PMN powders. With a simple mixed-oxide route, PT powders were prepared from PbO (99.9%) and TiO₂ (99.9%) starting powders. These powders were ball-milled and calcined at $600\,^{\circ}\text{C}$ for 1 h.

The (1-x)Pb $(Mg_{1/3}Nb_{2/3})O_3-(x)$ PbTi O_3 ceramics were then prepared from starting PMN and PT powders by the mixed-oxide method. After mixing the powders by the ballmilling method and drying process, the mixed powders were pressed hydraulically to form disc-shaped pellets 10 mm in diameter and 2 mm thick, with 3 wt% polyvinyl alcohol as a binder. The pellets were placed on the alumina powderbed inside alumina crucible and surrounded with atmosphere powders of the same composition. Finally, for optimization purposes the pellets were sintered at temperatures between 1220 and 1240 °C for 2 h. Optimum sintering conditions for all ceramics were established by identifying the conditions for maximizing both the bulk density and the yield of perovskite. However since the PMN-PT compositions having high PT content in the range $0.6 \le x \le 0.9$ could not be fabricated in a bulk form of high density, these compositions could not be characterized any further for the rest of the study. Their comparatively large c/a values, which give rise to serious internal stress, are responsible for the frequent crack

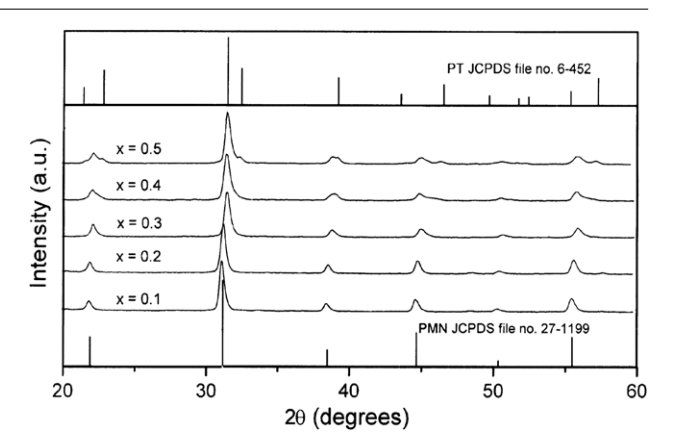


Figure 1. XRD diffraction patterns of the sintered (1 - x)PMN-(x)PT ceramics.

developments around the phase transition temperature during the cooling of these sintered samples. In the present study, only compositions in the pseudo-binary system (1 - x)PMN– xPT (0.1 $\leq x \leq$ 0.5) have been successfully fabricated from the calcined (1 - x)PMN-xPT powders, employing a normal sintering method, i.e. the pressureless sintering technique. Similar optimum sintering conditions of 1240 °C for 2 h with 15 °C min⁻¹ were observed in samples at compositions of x between 0.1 to 0.3 while for compositions with PT content of x = 0.4 and 0.5 the optimum condition was found at 1220 °C for 2 h with 15 °C min⁻¹ [25]. The phase-formation of the sintered ceramics was studied by the x-ray diffraction (XRD) technique. The densities of sintered specimens were measured by Archimedes method. The microstructure analyses were undertaken by scanning electron microscopy (SEM: JEOL Model JSM 840A). The grain size was determined from SEM micrographs by a linear intercept method.

Before studying the dielectric properties, the specimens were lapped to obtain parallel faces. After coating with silver paint as electrode at the faces, the specimens were heated at 750 °C for 12 min to ensure contact between the electrode and the surface of the ceramic. All the ceramics were then poled to a full remanent state prior to testing. A compressometer was constructed [19, 26, 27] to study the effects of the compressive stress on the dielectric properties of the ceramics. The dielectric properties were measured by LCR-meter (Instrek LCR-821). The room temperature (25 °C) capacitance and the dielectric loss tangent were obtained at a frequency of 1 kHz under compressive stress up to 230 MPa. The dielectric constant was then calculated from a parallelplate capacitor equation, e.g. $\varepsilon_r = Cd/\varepsilon_0 A$, where C is the capacitance of the specimens, d and A are, respectively, the thickness and the area of the electrode and ε_0 is the dielectric permittivity of vacuum (8.854 \times 10⁻¹² F m⁻¹).

3. Results and discussion

The XRD patterns of sintered ceramics with maximum perovskite phase and bulk density are presented in figure 1, where complete crystalline solutions of perovskite structure are formed throughout the composition range between x = 0.1 and 0.5. In general, only a (pseudo) cubic symmetry is observed at low values of PT concentration, in good

Table 1. Characteristics of Pl	MN-PT	ceramics	with o	ptimized	processing	conditions.
---------------------------------------	-------	----------	--------	----------	------------	-------------

					Stress-free dielectric properties	
Ceramic	Density ^a (g cm ⁻³)	Grain size range (μm)	Average grain size ^b (μm)	<i>T</i> _C (1 kHz) (°C)	$arepsilon_{ m r}$	tan δ
0.9PMN-0.1PT	7.98	0.42-3.66	2.07	45	10713	0.083
0.8PMN-0.2PT	7.94	0.44 - 3.02	2.02	100	2883	0.079
0.7PMN-0.3PT	7.86	0.41 - 2.80	1.72	150	1 976	0.045
0.6PMN-0.4PT	7.83	0.41 - 3.45	1.93	210	1 909	0.031
0.5PMN-0.5PT	7.78	0.48 - 3.72	2.11	260	1 375	0.022

^a The estimated precision of the density is $\pm 1\%$.

agreement with other workers [28, 29]. By the influence of PT, however, several peaks split for $x \ge 0.4$, indicating the development of tetragonal symmetry, consistent with earlier work on PMN-PT ceramics [9, 30]. As listed in table 1, density values are found to decrease slightly with x (in units of grams per centimetre cube the value decreases gradually from 7.98 in 0.9PMN-0.1PT to 7.78 in 0.5PMN-0.5PT). SEM-micrographs of fractured surfaces of all compositions are shown in figure 2. In general, similar microstructure characteristics are observed in these samples, i.e. uniformly sized grains with a high degree of grain close-packing. Almost no abnormal grain growth is observed. All ceramic compositions display very similar grain size range between 0.4 and $3.7 \mu m$. By applying the linear intercept method to SEM micrographs of polished and thermally etched specimens, mean grain sizes of about $1.72-2.11 \,\mu\text{m}$ are estimated for these samples as given in table 1. These characteristics indicate that dense perovskite-phase PMN-PT ceramics with uniform microstructure have been obtained. Since the physical and microstructure features of all ceramic compositions are not significantly different, these parameters should not play an important role in the composition-dependent dielectric properties under the compressive stress discussed in the following paragraphs.

The room temperature dielectric properties measured under stress-free condition are listed in table 1. It is clearly seen that the dielectric constant (ε_r) of (1-x)PMN-(x)PT ceramics decreases with increasing PT content. The dielectric constant decreases from 10713 in 0.9PMN-0.1PT to 1375 in 0.5PMN-0.5PT. In addition, a decreasing trend has been observed for the stress-free dielectric loss tangent (tan δ), which shows a decrease in value from 0.083 in 0.9PMN-0.1PT to 0.022 in 0.5PMN-0.5PT. This observation could be attributed to a high dielectric constant of PMN and a closer to ambient temperature T_C for PMN-PT compositions with higher PMN content [1,4,5]. Comparable stress-free dielectric properties have also been reported in earlier publications [2,5,29,30].

The experimental results of the compressive stress dependence of the dielectric properties during loading and unloading for the ceramics in the PMN-PT system are displayed in figures 3 and 4. For better comparison, the dielectric properties of each composition under stress are normalized to the stress-free values. Clearly, there is a considerable change in both the dielectric constant and the dielectric loss tangent when the compressive stress increases from 0 to 230 MPa and returning to stress-free condition. As

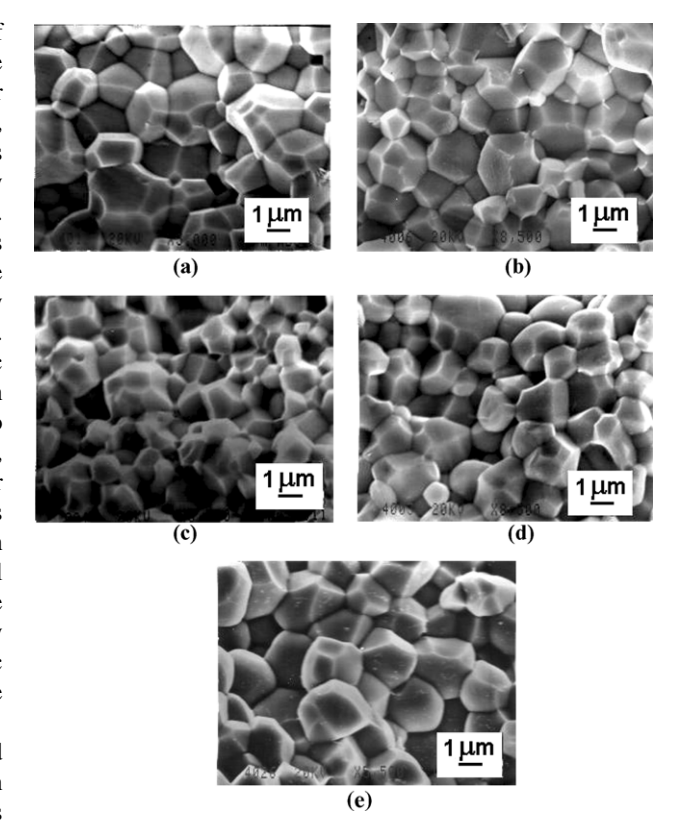


Figure 2. SEM micrographs of fracture surfaces of (1-x)PMN–(x)PT ceramics (a) 0.9PMN–0.1PT; (b) 0.8PMN–0.2PT; (c) 0.7PMN–0.3PT; (d) 0.6PMN–0.4PT and (e) 0.5PMN–0.5PT.

depicted in figure 3, the changes of the dielectric constant with the stress can be divided into two groups. For 0.9PMN–0.1PT ceramic, the dielectric constant decreases drastically with the stress. The dielectric constant decreases more than 70% when the stress reaches 230 MPa and only returns to slightly less than 50% of its original value when the stress is removed. The changing of the dielectric constant with increasing and decreasing stress does not follow the same path. On the other hand, for other PMN–PT ceramics, i.e. with x values of 0.2–0.5, the change is minimal. The dielectric constant is actually rather stable within this range of the stress. The dielectric constant of these compositions initially increases then decreases with very little difference in the dielectric constant between stress-free and maximum stress

^b The estimated precision of the average grain size is $\pm 1\%$.

^c Measured at 1 V mm⁻¹ (25 °C and 1 kHz).

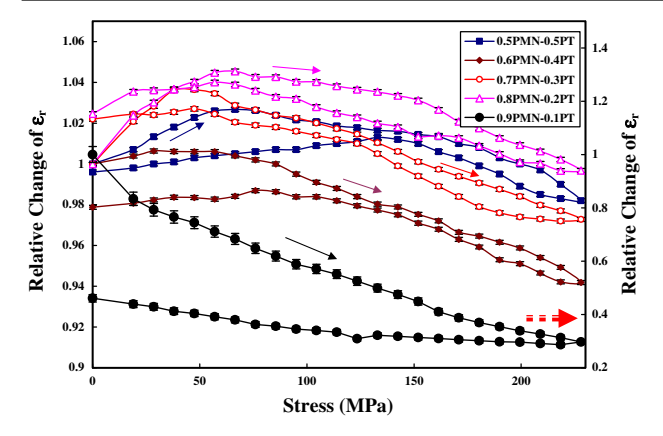


Figure 3. Relative changes of the dielectric constant (ε_r) with compressive stress for (1-x)PMN–(x)PT ceramics (measured at 25 °C and 1 kHz; secondary *Y*-axis is only for 0.9PMN–0.1PT and solid arrows indicate loading direction).

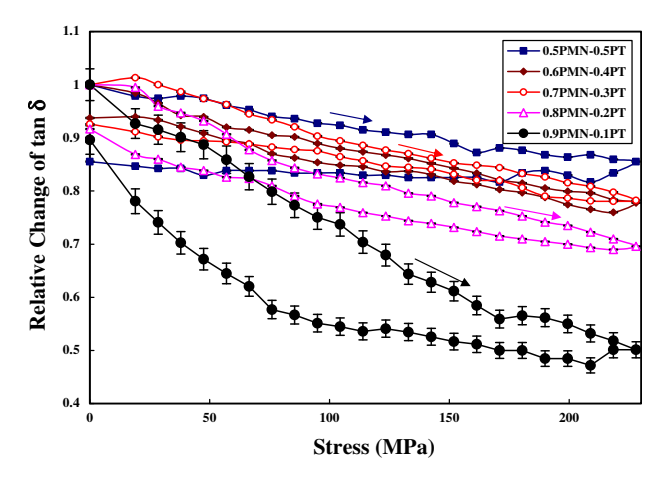


Figure 4. Relative changes of dielectric loss tangent $(\tan \delta)$ with compressive stress for (1 - x)PMN-(x)PT ceramics (measured at 25 °C and 1 kHz; solid arrows indicate loading direction).

conditions. In addition, the dielectric constants during loading and unloading are not significantly different.

Since the dielectric constant of the sample was measured through the capacitance, there is a change in sample capacitance due to the geometrical deformation under stress. The variation of the sample dielectric constant $(\Delta \varepsilon_r)$ can be expressed as $\varepsilon_r^* X^*((1+2\upsilon)/E)$, where X is the applied stress, υ is the Poisson's ratio and E is the Young's modulus [26, 31]. By applying the estimated values of $\upsilon \sim 0.3$ and $E \sim 100$ GPa for PMN–PT ceramics [7, 23, 24, 32] and ε_r given in table 1, it can be estimated that at the maximum stress of 230 MPa, the variation in the sample dielectric constant due to the geometrical deformation is <0.5%. Therefore, this variation should not be an important factor in the variation of the dielectric constant under stress seen in figure 3.

Figure 4 shows the results of the compressive stress dependence of the dielectric loss tangent. The dielectric loss tangent decreases monotonously with increasing the stress and then increases slightly when stress is removed. The dielectric loss tangent is also found to decrease considerably after a stress cycle. This is clearly seen in 0.9PMN–0.1PT ceramics, where the change in the dielectric loss tangent value is very significant, as it decreases about 50% at the maximum stress

and almost returns to its original value after a stress cycle. The changes in the other compositions are less significant with increasing PT content.

It is also noticed that the changes in the dielectric properties with the compressive stress obtained in this study are in parts similar to those for the (1-x)PMN-(x)PZT system in the earlier investigation [19]. By comparison, the 0.9PMN-0.1PT behaves more like PMN-rich compositions in that study, while the other PMN-PT compositions act more like the PZT-rich compositions. It should also be noted that the $T_{\rm C}$ range of 16–160 °C for the (1-x)PMN-(x)PZT system with x=0.1–0.7 [33, 34] is nearly similar to that of the PMN-PT ceramics used in this study, as listed in table 1. More importantly, it is interesting to observe that a mixture of different normal and relaxor ferroelectrics responds to the applied stress in a similar manner.

To understand these experimental results, at least qualitatively, various effects have to be considered. Normally, the properties of ferroelectric materials are derived from both the intrinsic contribution of domains and extrinsic contributions of re-polarization and growth of micro-polar regions [19–23]. When a compressive stress is applied to the ferroelectric materials, the domain structure in the materials will change to maintain the domain energy at a minimum; during this process some of the domains engulf other domains or change shape irreversibly. Under the applied stress, the domain structure of ferroelectric ceramics may undergo domain switching through non-180° domain walls, de-ageing, clamping of domain walls and stress induced decrease in the switchable part of spontaneous polarization [21, 23, 35].

The situation for the PMN-PT system is quite complex because this system is a mixing between the relaxor ferroelectric PMN and the normal ferroelectric PT. Therefore, there is a competing mechanism between the two types of materials, depending upon temperature and composition. Since 0.9PMN-0.1PT is a relaxor ferroelectric with $T_{\rm C}$ ~ 45 °C and the experiment was carried out at room temperature (\sim 25 °C) which is slightly below $T_{\rm C}$, the experimental observations, which show decreases in both dielectric constant and dielectric loss tangent with increasing stress, can be attributed to competing influences of the intrinsic contribution of the non-polar matrix and the extrinsic contribution of repolarization and growth of micro-polar regions. Since the dielectric response of both contributions is affected by the applied stress in an opposite way, the behaviour of 0.9PMN-0.1PT depends on the ratio between the micro-polar region and the non-polar matrix, in this case the non-polar matrix still dominates [21,22]. Hence, the dielectric responses of the 0.9PMN-0.1PT ceramic are observed to decrease significantly with increasing compressive stress, as seen in figures 3 and 4. Earlier works on PMN and 0.9PMN-0.1PT ceramics also reported a similar observation [22,23]. However, under stress as high as 230 MPa microcracks may develop, particularly in 0.9PMN-0.1PT, which in turn could lead to a significant change in the dielectric properties. Therefore, an additional experiment was carried out to investigate the existence of the microcracks. The stressed specimens were annealed at 300 °C for 3 h [36], then poled at the same condition used earlier. The dielectric properties were re-measured under a stress-free condition. The results showed a full recovery of the dielectric

properties, within experimental errors. This indicated that there were no microcracks in the stressed specimens.

For the other PMN–PT compositions with higher $T_{\rm C}$, the extrinsic contribution of re-polarization and growth of micropolar regions becomes dominant. When the compressive stress is applied in the direction parallel to the poling direction, the stress will move some of the polarization away from the poling direction resulting in a change in domain structures [20]. This change increases the non-180° domain wall density. Hence increase in the dielectric constant is observed. The de-ageing mechanism, which also increases the dielectric constant, is also expected to play a role here. After poling, ceramics undergo an ageing process during which some of the domain walls become pinned by impurities and structural imperfections. When a large enough stress is applied to the aged samples, it causes structural changes and redistribution of impurities [21]. As a result, the domain walls that were pinned during ageing can become active again. This de-ageing can increase dielectric responses [20, 23]. Therefore, a combination of the domain switching and the de-ageing mechanisms is believed to be a reason for the slight increase in the dielectric constant during low-stress application. With further increase in the stress, the stress clamping of domain walls, which results in a decrease of domain wall mobility, and the stress induced decrease in the switchable part of spontaneous polarization are expected to play a role in the decrease in the dielectric constant [21,23,35]. Therefore, the dielectric constant of these compositions is seen to be rather stable with the applied stress, as seen in figure 3. Similar observation has also been reported in soft PZT [20,23].

The cause of the stress dependence of the dielectric loss tangent is a little more straightforward than that of the dielectric constant. As depicted in figure 4, the clamping of the domain walls under the compressive stress results in a decrease of domain wall mobility and reduces the dielectric loss tangent [21]. This is a reversible effect with the domain wall mobility returning to near original values when the applied stress is removed, as seen in figure 4 that dielectric loss tangents return to near original values after a stress cycle. In addition, a significant decrease in the dielectric constant after a full cycle of stress application has been observed, particularly in 0.9PMN–0.1PT, and attributed to the stress induced decrease in the switchable part of the spontaneous polarization at high stress [23,35].

4. Conclusions

In this study, the dielectric properties of (1 - x)Pb(Mg_{1/3} Nb_{2/3})O₃–(x)PbTiO₃ or (1 - x)PMN–(x)PT (x = 0.1–0.5) ceramics prepared by a conventional mixed-oxide method are measured under compressive stress from 0 to 230 MPa. Phase formation behaviour and microstructure features of these ceramics are studied by an XRD and SEM methods, respectively. Perovskite-phase PMN–PT ceramics with homogeneous microstructure are obtained. The dielectric properties of 0.9PMN–0.1PT ceramic are found to decrease significantly with compressive stress, while the changes are not as significant in the other PMN–PT ceramic compositions. In addition, the dielectric properties are considerably lowered after a stress cycle. The change in dielectric properties with the applied stress is attributed to competing influences of intrinsic

and extrinsic contributions. The observations are then mainly interpreted in terms of domain switching through non- 180° domain walls, de-ageing, clamping of domain walls and the stress induced decrease in the switchable part of spontaneous polarization.

Acknowledgments

This work is supported by the Thailand Research Fund (TRF). Additional support from the Faculty of Science and Graduate School of Chiang Mai University are gratefully acknowledged. The authors would also like to express their gratitude to Aurawan Udomporn for help in sample preparation and characterization.

References

- [1] Xu Y H 1991 Ferroelectric Materials and Their Applications (Amsterdam: North Holland)
- [2] Moulson A J and Herbert J M 2003 Electroceramics: Materials, Properties, Applications (Chichester: Wiley)
- [3] Haertling G H 1999 J. Am. Ceram. Soc. 82 797
- [4] Cross L E 1987 Ferroelectrics 76 241
- [5] Jang S 1979 PhD Thesis Pennsylvania State University
- [6] Uchino K 1997 Piezoelectric Actuators and Ultrasonic Motors (Boston, MA: Kluwer)
- [7] Viehland D, Li J, McLaughlin E, Powers J, Janus R and Robinson H 2004 J. Appl. Phys. 95 1969
- [8] Shrout T R, Chang Z, Kim N and Markgraf S 1990 Ferroelectr. Lett. Sect. 12 63
- [9] Viehland D, Kim M, Xu Z and Li J 1995 Appl. Phys. Lett. 67 2471
- [10] Smolenskii G and Agranovskaya A 1960 Sov. Phys. Solid State 1 1429
- [11] Randall C, Barber D and Whatmore R 1987 J. Microsc. 45 275
- [12] Dai X, Xu Z and Viehland D 1994 Phil. Mag. B 70 33
- [13] Kuwata J, Uchino K and Nomura S 1982 Japan. J. Appl. Phys. 21 1298
- [14] Park S and Shrout T R 1997 J. Appl. Phys. 82 1804
- [15] Viehland D and Powers J 2001 Appl. Phys. Lett. 78 3112
- [16] Stansfield D 1991 *Underwater Electroacoustic Transducers* (Bath, UK: Bath University Press)
- [17] Mitrovic M, Carmen G P and Straub F K 2001 Int. J. Solids Struct. 38 4357
- [18] Zhou D, Kamlah M and Munz D 2005 J. Euro. Ceram. Soc. 25 425
- [19] Yimnirun R, Ananta S, Meechoowas E and Wongsaenmai S 2003 J. Phys. D: Appl. Phys. 36 1615
- [20] Zhang Q M, Zhao J, Uchino K and Zheng J 1997 J. Mater. Res. 12 226
- [21] Yang G, Liu S F, Ren W and Mukherjee B K 2000 Proc. SPIE Symp. on Smart Struct. Mater. 3992 103
- [22] Steiner O, Tagantsev A K, Colla E L and Setter N 1999 J. Euro. Ceram. Soc. 19 1243
- [23] Zhao J and Zhang Q M 1996 Proc. IEEE Int. Symp. Appl. Ferroelectr. 2 971
- [24] Zhao J, Glazounov A E and Zhang Q M 1999 Appl. Phys. Lett. 74 436
- [25] Udomporn A 2004 PhD Thesis Chiang Mai University
- [26] Yimnirun R, Moses P J, Meyer R J and Newnham R E 2003 Rev. Sci. Instrum. 74 3429
- [27] Yimnirun R, Ananta S, Ngamjarurojana A and Wongsaenmai S 2005 Appl. Phys. A 81 1227
- [28] Kong L B, Ma J, Zhu W and Tan O K 2002 *Mater. Res. Bull.* 37 23
- [29] Liou Y C 2003 Mater. Sci. Eng. B 103 281
- [30] Brown L F, Carlson R L, Sempsrott J M, Standford G T and Fitzgerald J J 1997 Proc. IEEE Ultrason. Symp. 1 561

- [31] Preu P and Haussuhl S 1983 Solid State Commun. **45** 619
- [32] Viehland D and Powers J 2001 J. Appl. Phys. **89** 1820
- [33] Yimnirun R, Ananta S and Loaratanakul P 2004 *Mater. Sci. Eng.* B **112** 79
- [34] Yimnirun R, Ananta S and Loaratanakul P 2005 J. Euro. Ceram. Soc. 25 3225
 [35] Yimnirun R, Loasiritaworn Y and Wongsaenmai S 2006 J.
- Phys. D: Appl. Phys. 39 759
 [36] Liao J, Jiang X P, Xu G S, Luo H S and Yin Q R 2000 Mater.
 Charact. 44 453

Effects of Sintering Condition on Phase Formation, Microstructure and

Dielectric Properties of Lead Titanate Ceramics

R. Wongmaneerung, R. Yimnirun and S. Ananta

Department of Physics, Faculty of Science, Chiang Mai University, Chiang Mai

50200, Thailand

ABSTRACT

PbTiO₃ ceramics have been prepared by two different processing methods:

conventional (or single-stage) and two-stage sintering. Effects of designed

sintering conditions on phase formation, densification, microstructure and

dielectric properties of the ceramics were characterized via X-ray diffraction

(XRD), Archimedes density measurement, scanning electron microscopy

(SEM) and dielectric measurement, respectively. The potentiality of a two-

stage sintering technique as a low-cost and simple ceramic fabrication

method to obtain highly dense and pure lead titanate ceramics was

demonstrated. It has been found that, under suitable two-stage sintering

conditions, dense perovskite PT ceramics can be successfully achieved with

better dielectric properties than those of ceramics from a single-stage

sintering technique.

Keywords: Lead titanate; PbTiO₃; Perovskite ceramics; Sintering;

Microstructure; Dielectric Properties

1. INTRODUCTION

Being one of the lead-based perovskites, lead titanate (PbTiO₃ or PT) is of interest as a component in commercial electroceramic materials. In addition, PT when combined with other oxides can form a series of ferroelectric materials that exhibit many of the most desirable dielectric, piezoelectric and pyroelectric properties for use in electronic devices at high frequency and high temperature, such as infrared sensors, microactuators, capacitors and hydrophones [1-3]. The most important properties of perovskite PT ceramics are high Curie temperature (~ 490 °C), large mechanical-quality factor and pyroelectric coefficient [4,5]. However, pure and dense PT ceramics are regarded to be one of the most difficult lead-based perovskite ferroelectric ceramics to produce [6]. PT ceramic is mechanically weak due to large distortion of the tetragonal phase at room temperature which is characterized by the ratio between the lattice parameters (c/a, hereafter called tetragonality, ~ 1.06 [6,7]). Apart from general problems of PbO volatilization and associated high porosity, the stress induced by cooling through the phase transition can create cracking in bulk ceramics. In addition, it is difficult to pole the ceramics with low resistivity (10⁷-10⁸ cm) [8].

To overcome these problems, several techniques have been introduced, such as utilizing ultrafine powders, using additives, employing spark-plasma sintering and carrying out appropriate milling and sintering conditions [8-13]. All these techniques are aimed at reducing the lattice tetragonality of the bulk ceramics, even though they inevitably affect the phase formation, structure and electrical properties of materials in different ways. Amongst all the approaches reported so far, most attention has been

concentrated on the use of additives and powder processing, whereas investigations on modified sintering techniques have not been widely carried out [13,14].

Therefore, in this work, a two-stage sintering method has been developed to resolve these problems. With this new scheme, instead of using a single, high firing temperature (of up to $1225\,^{\circ}\text{C}$) [13] where the degree of PbO volatilization affects the stoichiometry of the product by forming a pyrochlore phase, in addition to a perovskite phase, two moderate temperatures (T_1 and T_2 with a constant dwell time of 2 h at each stage) were adopted. The aim of this study was to investigate the influence of these two ceramic processing methods (single- and two-stage sintering) on phase formation, densification, microstructure and dielectric properties of PbTiO₃ ceramics.

2. MATERIALS AND METHODS

Commercially available powders of PbO and TiO₂ (anatase form), (Fluka, > 99% purity) were used as starting materials. A simple mixed oxide synthetic route was employed to synthesize PbTiO₃ powders. The mixing process was carried out by ball-milling a mixture of raw materials for 24 h with corundum media in isopropyl alcohol (IPA). After wet-milling, the slurry was dried at 120 °C for 2 h, sieved and calcined in a closed alumina crucible, with the optimum calcination conditions determined by the XRD method (600 °C for 2 h with heating/cooling rates of 5 °C/min [15]). Ceramic fabrication was achieved by adding 3 wt% polyvinyl alcohol (PVA) binder, prior to pressing as pellets (15 mm in diameter and 1.0 to 1.3 mm thick) in a pseudo-uniaxial die

press at 100 MPa. Each pellet was placed in an alumina crucible together with an atmosphere powder of identical chemical composition. After the binder burn out at 500 °C for 1 h, sintering was carried out with a dwell time of 2 h at each step, with constant heating/cooling rates of 1 °C/min [13] applied (Fig. 1). Variation of the firing temperature between 1150 and 1250 °C was carried out for the single-stage sintering samples. Three sets of the first sintering temperature (T₁) were assigned for the two-stage sintering case: 700, 800 and 900 °C. Variation of the second sintering temperature (T₂) between 1000 °C and 1250 °C was carried out for each case.

Densities of the final sintered products were determined by using the Archimedes principle. Sintered ceramics were examined by room temperature X-ray diffraction (XRD; Siemens-D500 diffractometer) using CuK radiation to identify the phase formed. The lattice parameters and tetragonality factor (*c/a*) of the sintered ceramics were calculated from the XRD patterns [16]. The microstructural development was characterized using a JEOL JSM-840A scanning electron microscopy (SEM), equipped with an energy dispersive X-ray (EDX) analyzer. Mean grain sizes of the sintered ceramics were subsequently estimated by employing the linear intercept method [17]. In order to evaluate the dielectric properties, dense ceramics were polished to form flat, parallel faces (14 mm in diameter and 0.8 mm thick). The samples were then coated with silver-paste electrodes which were fired on both sides of the samples at 700 °C for 1 h. The dielectric properties were measured at a frequency of 1 MHz using a HIOKI 3532-50 LCR meter, on cooling through the transition range (500 to 25 °C) with a rate of 5 °C/min.

3. RESULTS AND DISCUSSION

X-ray diffraction patterns of the PT ceramics sintered at various conditions are displayed in Figs. 2 and 3, indicating the formation of both perovskite and impurity phases in each case. The strongest reflections in the majority of all XRD traces indicate the formation of the PbTiO₃ perovskite phase of lead titanate which could be matched with JCPDS file no. 6-452, in agreement with other works [11-13]. To a first approximation, this major phase has a tetragonal perovskite-type structure in space group *P4/mmm* (no. 123) with cell parameters a = 389.93 pm and c = 415.32 pm [18]. For the singly sintered PT ceramics, additional weak reflections are found in the samples sintered above 1175 °C (marked by ▼ in Fig. 2), which correlate to the starting precursor PbO (JCPDS file no.77-1971) [19]. This observation could be attributed mainly to the poor mixing of the employed powders derived from the ball-milling technique. The relative amounts of perovskite and minor phase present in each sintered ceramic were calculated from the intensities of the major X-ray reflections from the respective phases. In this connection, the following approximation was adopted, as in the earlier PMN and PFN studies [14]:

perovskite phase (wt-%) =
$$I_P/(I_P + I_M) \times 100$$
 (1)

Here I_P and I_M refer to the intensities of the {110} perovskite and {111} minor phase peaks, respectively, these being the most intense reflections in the XRD patterns of both phases. For the purposes of estimating the concentration of minor phase present, eqn (1) has been applied to the diffraction patterns obtained (numerical data are presented in Tables 1 and 2).

More interestingly, a single phase of perovskite PT is found in all the doubly sintered samples (Fig. 3), in contrast to the observations for the singly sintered samples. No evidence of pyrochlore phase of PbTi₃O₇ composition earlier reported by Udomporn and Ananta and Tartaj et al. [8,14] was found, nor was there any evidence of other second phases [21] being present. This could be due to the lower firing temperature of the doubly sintered samples as compared to the singly sintered ceramics, leading to a smaller degree of lead losses and consequently avoiding the pyrochlore formation, while a sufficient amount of energy required for ceramic densification still to be reached was provided by the longer holding time, in agreement with other works [14,22,23]. However, many other factors come into play, e.g. homogeneity of materials, reactivity of starting powders, and processing variables. These XRD results clearly show that, in general, the different processing methods used for preparing PT ceramics gave rise to a different phase formation in the sintered materials. The absence of minor phase in doubly sintered samples was related to the more reactive process used [14].

Tables 1 and 2 also present tetragonality factor (*c/a*), relative density and average grain size of singly- and doubly-sintered samples, respectively. Generally, it is evident that as the sintering temperature increases, the density of almost all the samples increases. However, it can be seen that the sintering behaviour of singly and doubly sintered PT ceramics was dissimilar. Doubly sintered ceramics reached a maximum density of ~ 97% at 900/1150 °C or 900/1200 °C. On the other hand, singly sintered samples exhibit less densification, and a temperature of 1225 °C was required to reach a densification level of ~ 94%. The densification of all materials slightly

decreased at temperatures higher than those of the maximum density, accompanied by a significant increase of weight loss (~ 2-5%). By comparison with singly sintered PT ceramics, lower values of tetragonality (*c/a*) are found in all double sintered case, indicating lower internal stress in these sintered samples.

Microstructural features of PT samples singly sintered at different temperatures for 2 h with heating/cooling rates of 1 °C/min are shown in Fig. 4. It was found that the samples subjected to low sintering temperature e.g. 1150 °C eventually burst into pieces because of the internal anisotropic stress caused by the phase transition in the ceramics as can be confirmed by the SEM images showing a loose formation of large grains (Fig. 4(a) and (b)), in agreement with high values of *c/a* given in Table 1. Additionally, average grain sizes were found to increase with the sintering temperature. For higher temperature treatments, a pronounced second phase is segregated at the grain boundaries. The EDX spectra indicated that there was more Pb and less Ti in the bright region than in the dark region, as shown in Fig. 4 (b-d). The observation of these (second phase) layers could be attributed to a liquid phase formation during the sintering process as proposed by many researchers [24,25].

In addition, a combination of SEM and EDX techniques has demonstrated that small amounts of nano-sized (~ 1.7 -2.5 nm) spherical TiO₂ inclusions (brighter phase) exist on the surface of perovskite PT grains in some samples, as shown in Fig. 4(b) and (c), similar to those found by Takeuchi *et al.* [26]. The existence of a discrete TiO₂ phase points to the expected problem of poor homogeneity of the samples arising from PbO

volatilization after being subjected to prolonged heating, although the concentration is too low for XRD detection.

Representative microstructures for doubly sintered PT ceramics are given in Fig. 5. The first sintering temperature was designed at 700, 800 and 900 °C, for constant dwell time and heating/cooling rates of 2 h and 1 °C/min at each stage, while the second sintering temperature was varied from 1100 °C to 1200 °C. It is seen that a uniform grain shape of typical perovskite ceramics [9,22,23] is observed, with sizes in the range of 0.4-2.0 m. It should be noted that the average grain size of the doubly sintered PT ceramics is < 2.0 m, which is less than the critical value of 3 m reported by several workers [11,26,27]. Here, it is believed that smaller grains with random orientations result in lower internal stress in sintered samples because they compensate the anisotropy of thermal expansion coefficients.

By comparison with singly sintered PT ceramics, almost clean microstructures with high uniformity, denser angular grain-packing and more homogeneity are generally observed in doubly sintered PT samples. These microstructures are typical of a solid-state sintering mechanism. In the present study (Fig. 5 and Table 2), the microstructural features of the doubly sintered PT ceramics with various second sintering temperatures ranging from 1050 to 1200 °C are not significantly different. However, it should be noted that higher angular grains were evidenced for higher second sintering temperature (see Fig. 5 (b), (d) and (f)). The observation that the sintering temperature effect may also play an important role in obtaining a high angularity in the grains of perovskite ceramics is also consistent with other similar systems [22,23]. Moreover, an abnormal grain growth probably due to the inhibition of the

normal grain growth mechanism during doubly sintering process [14] was also found in some samples, as shown in Fig. 5(c). It is also of interest to point out that evidence has been found for the existence of microcracks (arrowed) along the grain boundaries of the samples sintered at lower second sintering temperatures (Fig. 5(c) and (e)), in agreement with other works [9,26,28].

Interestingly, only the samples sintered at 700/1100-1200 °C, 800/1050-1200 °C or 900/1050-1200 °C with the highest relative density and smallest average grain size of about 95-97% and 0.3-1.9 m, respectively, remained unbroken. It may be simply assumed that the ceramics consisting of very fine grains have less elastic strain energy than the ceramics with significantly large grains (Tables 1 and 2). Consequently, the experimental work carried out here suggests that the optimum conditions for forming the highly dense PT ceramics in this work are double-sintering temperatures at 700-900/1100-1200 °C, 2 h dwell time, and 1 °C/min heating/cooling rates. The different microstructure evolution of PT ceramics confirms the importance of the processing method. More importantly, considered from the perovskite content and microstructure of PT ceramics sintered by two different methods, the doubly sintered method was clearly preferable for obtaining dense perovskite PT ceramics. The following discussion on the dielectric properties of the PT ceramics obtained in this study would further support the advantage of the doubly sintering method.

The dielectric properties of the PT samples sintered with different techniques are also compared in Table 3, as well as in Fig. 6. The Curie temperatures are about the same for all samples measured whilst the dielectric properties of both sets of the sintered PT ceramics seem to be

different. As listed in Table 3, the room temperature dielectric properties of the two sets of ceramics are not significantly different. The values of dielectric constant in the order of 200 are slightly higher than those reported earlier [9,29]. However, the high temperature dielectric properties of the doubly sintered PT samples are noticeably higher than those of singly sintered PT sample, as seen in inset of Fig. 6. As mentioned earlier, the reason for this is the high amount of secondary phase present in the singly sintered PT ceramics. In addition, the presence of a PbO-rich phase (as observed in Fig. 4 (b-d)), with low dielectric constant, might be forming a continuous layer between grains, hence decreasing the dielectric constant of the singly sintered PT ceramics [13,24,30]. The secondary phases in singly sintered PT are interconnected at grain boundaries and, as suggested by Wang and Schulze [24], exert more influence on the dielectric properties than when they are isolated.

Grain sizes also play a role in the difference in the dielectric properties, especially the dielectric constant. As clearly seen in Tables 1 and 2 (as well as Figs. 4 and 5), the larger grain size in the singly sintered ceramics would lead to lower dielectric constant than that of the doubly sintered ceramics. This relation is well established in several ceramic perovskite systems e.g. BaTiO₃ [31], PZT [32,33], PMN [22,34] and PFN [23].

The different microstructure and the different amount of secondary phases present in singly and doubly sintered PT ceramics strongly influences the dielectric properties of these materials, leading to superior electrical behaviour in doubly sintered PT ceramics. Moreover, this study demonstrated that the dielectric properties of PT ceramics are also influenced by

microstructural features especially the phase compositions at grain boundaries, microcracks and densification mechanism rather than by only pyrochlore phase or by grain size itself.

Although a disadvantage of the proposed two-stage sintering method is a greater time-requirement, the significant reduction in firing temperature is a positive development, particularly with regard to the drive towards electrodes of lower cost [1-3]. In general, these PT ceramics exhibit complex microstructures which are a result of variation in grain size and orientation; variation in chemical homogeneity; and the presence and distribution of additional minor phase, pores and (micro) cracks. These factors, which are strongly influenced by the sintering conditions, have an important effect on the dielectric properties of materials and their reproducibility.

4. CONCLUSION

The processing method used for preparing PT ceramics greatly influences the final properties of the ceramics. Even though the simple mixed-oxide method employing a conventional ball-milling was used, this work demonstrated that it was possible to obtain rather dense PT ceramics with homogeneous microstructure by the two-stage sintering technique. It has been shown that, under suitable sintering conditions, the phase formation and densification of the ceramics are better than those obtained from the single-stage sintering. Reductions in the maximum required sintering temperature are possible as compared to the single-stage sintering.

ACKNOWLEDGEMENT

This work was supported by the Thailand Research Fund (TRF), the Faculty of Science and the Graduate School of Chiang Mai University.

REFERENCES

- [1] B. Jaffe, W.R. Cook, H. Jaffe, Piezoelectric Ceramics, Academic Press, New York, 1971.
- [2] G.H. Haertling, J. Am. Ceram. Soc.82 (1999) 797.
- [3] A.J. Moulson, J.M. Herbert, Electroceramics, 2nd ed., Wiley, Chichester, 2003.
- [4] T. Takahashi, Am. Ceram. Soc. Bull. 69 (1990) 691.
- [5] L.E. Cross, Mater. Chem. Phys. 43 (1996) 108.
- [6] G. Shirane, S. Hoshino, J. Phys. Soc. Jpn. 6 (1951) 265.
- [7] G. Shirane, R. Pepinsky, B.C. Frazer, Acta Crystallogr. 9 (1956) 131.
- [8] H. Takeuchi, S. Jyomura, E. Yamamoto, Y. Ito, J. Acoust. Soc. Am. 72 (1882) 1114.
- [9] L.B. Kong, W. Zhu, O.K. Tan, J. Mater. Sci. Lett. 19 (2000) 1963.
- [10] T. Suwannasiri, A. Safari, J. Am. Ceram. Soc. 76 (1993) 3155.
- [11] T. Takeuchi, M. Tabuchi, I. Kondoh, N. Tamari, H. Kageyama, J. Am. Ceram. Soc. 83 (2000) 541.
- [12] J.S. Forrester, J.S. Zobec, D. Phelan, E.H. Kisi, J. Solid State Chem. 177 (2004) 3553.
- [13] A. Udomporn, K. Pengpat, S. Ananta, J. Eur. Ceram. Soc. 24(2004) 185.
- [14] S. Ananta, N.W. Thomas, J. Eur. Ceram. Soc. 19 (1999) 2917.
- [15] A. Udomporn, S. Ananta, Mater. Lett. 58 (2004) 1154.
- [16] H. Klug, L.E. Alexander, X-ray Diffraction Procedures for Polycrystalline and Amorphous Materials, 2nd ed., Wiley, New York, 1974.
- [17] R.L. Fullman, Trans. AIME. 197 (1953) 447.

- [18] JCPDS-ICDD Card no. 6-452, International Centre for Diffraction Data, Newtown Square, PA, 2000.
- [19] JCPDS-ICDD Card no. 77-1971, International Centre for Diffraction Data, Newtown Square, PA, 2000.
- [20] J. Tartaj, C. Moure, L. Lascano, P. Durán, Mater. Res. Bull. 36 (2001) 2301.
- [21] M.L. Calzada, M. Alguero, L. Pardo, J. Sol-Gel Sci. Technol. 13 (1998) 837.
- [22] S. Ananta, N.W. Thomas, J. Eur. Ceram. Soc. 19 (1999) 629.
- [23] S. Ananta, N.W. Thomas, J. Eur. Ceram. Soc. 19 (1999) 1873.
- [24] H.C. Wang, W.A. Schulze, J. Am. Ceram. Soc. 73 (1990) 825.
- [25] S.M. Gupta, A.R. Kulkarni, J. Mater. Res. 10 (1995) 953.
- [26] T. Takeuchi, M. Takahashi, K. Ado, N. Tamari, K. Ichikawa, S. Miyamoto,M. Kawahara, M. Tabuchi, H. Kageyama, J. Am. Ceram. Soc. 84 (2001)2521.
- [27] Y. Matsuo, H. Sasaki, J. Am. Ceram. Soc. 49 (1966) 229.
- [28] S.R. Dhage, Y.B. Khollam, H.S. Potdar, S.B. Deshpande, B.D. Sarwade, D.K. Date, Mater. Lett. 56 (2002) 564.
- [29] S. Chattopadhyay, P. Ayyub, V.R. Palkar, M. Multani, Phys. Rev. B 52 (1995) 13177.
- [30] M. Villegas, A.C. Caballero, M. Kosec, C. Moure, P. Duran, J.F. Fernandez, J. Mater. Res. 14 (1999) 891.
- [31] A. Yamaji, Y. Enomoto, K. Kinoshita, T. Murakami, J. Am. Ceram. Soc. 60 (1977) 97.
- [32] B.M. Jin, J. Kim, S.C. Kim, Appl. Phys. A-Mater. 65 (1997) 53.

[33] W. Cao, C.A. Randall, J. Phys. Chem. Solids. 57 (1996) 1499.

[34] S.L. Swartz, T.R. Shrout, W.A. Schulze, L.E. Cross, J. Am. Ceram. Soc.67 (1984) 311.

Table Captions

- Table 1 Physical properties of singly sintered PT ceramics
- Table 2 Physical properties of doubly sintered PT ceramics
- Table 3 Dielectric Properties (at 1 MHz) of PT ceramics sintered at various conditions.

Figure Captions

- Fig. 1 A two-stage method sintering profile.
- Fig. 2 XRD patterns of PT ceramics singly sintered at various temperatures.
- Fig. 3 XRD patterns of PT ceramics doubly sintered at various conditions, with the first sintering temperature (T₁) at 700, 800 and 900 °C.
- Fig. 4 SEM micrographs of PT ceramics singly sintered at (a) 1150 (b) 1175 (c) 1200 and (d) 1225 °C.
- Fig. 5 SEM micrographs of PT ceramics doubly sintered at (a) 700/1100 (b) 700/1200 (c) 800/1100 (d) 800/1200 (e) 900/1100 and (f) 900/1200 °C.
- Fig. 6 Variation with temperature of (a) relative permittivity (r) and (b) dissipation factor (tan) at 1 MHz for PT ceramics sintered at various conditions (inset: relative permittivity vs temperature from 400 °C to 500 °C).

Table 1 Physical properties of singly sintered PT ceramics

Sintering	Perovskite	Tetragonality	Relative	Grain size
Temperature	phase	(c/a)	density	range (Mean) [*]
(°C)	(%)		(%)	(m)
1150	100	1.064	87	2.5-15.0 (6.5)
1175	100	1.064	89	8.0-26.5 (13)
1200	99.3	1.063	92	12.0-40.0 (29)
1225	90.1	1.063	94	20.0-65.0 (36)
1250	89.2	1.063	93	41.0-83.0 (52)

^{*}The estimated precision of the grain size is ± 10%

Table 2 Physical properties of doubly sintered PT ceramics

T ₁	T ₂	Perovkite	Tetragonality	Relative	Grain size
(°C)	(°C)	phase	(c/a)	density	range
		(%)		(%)	(Mean) [*]
					(m)
700	1000	-	-	-	-
700	1050	-	-	-	-
700	1100	100	1.058	96	0.3-0.5 (0.3)
700	1150	100	1.060	96	0.3-1.2 (0.8)
700	1200	100	1.062	96	0.4-1.7 (1.3)
700	1250	-	-	-	-
800	1000	-	-	-	-
8	1050	100	1.064	5	1.0-2.2 (1.6)
8	1100	100	1.061	6	0.5-3.3 (1.9)
8	1150	100	1.060	6	1.0-2.7 (1.8)
8	1200	100	1.062	6	0.6-1.7 (1.2)
800	1250	-	-	-	-
900	1000	-	-	-	-
900	1050	100	1.060	96	0.4-2.2 (1.2)
900	1100	100	1.060	96	0.7-1.5 (1.1)
900	1150	100	1.057	97	0.6-1.9 (0.8)
900	1200	100	1.061	97	1.0-2.2 (1.5)
900	1250	100	-	-	-

^{*}The estimated precision of the grain size is ± 10%

⁻ Data are not available because the samples were too fragile for the measurements.

Table 3 Dielectric Properties (at 1 MHz) of PT ceramics sintered at various conditions.

	Sintering Condition (°C for 2 h)				
Dielectric Properties	Single	Double (T ₁ /T ₂)			
(1 MHz)	1225	700/1200	800/1200	900/1200	
e _r (25 °C)	243	209	255	209	
tan d (25 °C)	0.01	0.05	0.03	0.03	
$\mathbf{e}_{\mathrm{r,max}}$	7680	8993	8322	8198	
tan _{max}	1.07	1.00	1.10	0.95	
T_{c}	482	484	484	484	

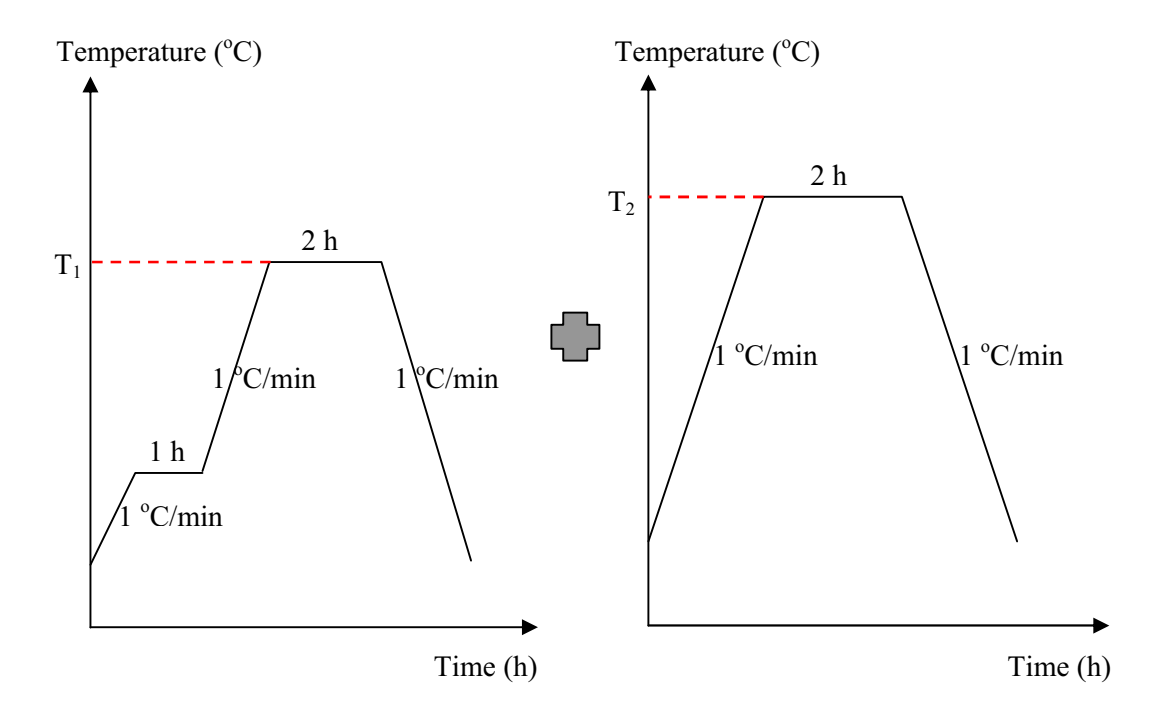


Fig. 1 A two-stage method sintering profile.